SANDIA REPORT

SAND2007-5138
Unlimited Release
Printed March 2008

3X-100 Blade Field Test

Jose R. Zayas and Wesley D. Johnson

Prepared by
Sandia National Laboratories
Albuquerque, New Mexico 87185 and Livermore, California 94550

Sandia is a multiprogram laboratory operated by Sandia Corporation,
a Lockheed Martin Company, for the United States Department of Energy's
National Nuclear Security Administration under Contract DE-AC04-94AL85000.

Issued by Sandia National Laboratories, operated for the United States Department of Energy by Sandia Corporation.

Available to DOE and DOE contractors from
U.S. Department of Energy
Office of Scientific and Technical Information
P.O. Box 62
Oak Ridge, TN 37831

Telephone: (865) 576-8401
Facsimile: (865) 576-5728
E-Mail: reports@adonis.osti.gov
Online ordering: http://www.osti.gov/bridge

Available to the public from
U.S. Department of Commerce
National Technical Information Service
5285 Port Royal Rd.
Springfield, VA 22161

Telephone: (800) 553-6847
Facsimile: (703) 605-6900
E-Mail: orders@ntis.fedworld.gov
Online order: http://www.ntis.gov/help/ordermethods.asp?loc=7-4-0#online

SAND2007-5138
Unlimited Release
Printed March 2008

3X-100 Blade Field Test

Jose R. Zayas and Wesley D. Johnson
Wind Energy Technology Department
Sandia National Laboratories
P.O. Box 5800
Albuquerque, NM 87185-0708

Abstract

In support of a Work-For-Other (WFO) agreement between the Wind Energy Technology Department at Sandia National Laboratories and 3TEX, one of the three Micon 65/13M wind turbines at the USDA Agriculture Research Service (ARS) center in Bushland, Texas, has been used to test a set of 9 meter wind turbine blades, manufactured by TPI composites using the 3TEX carbon material for the spar cap. Data collected from the test has been analyzed to evaluate both the aerodynamic performance and the structural response from the blades. The blades' aerodynamic and structural performance, the meteorological inflow and the wind turbine structural response has been monitored with an array of 57 instruments: 15 to characterize the blades, 13 to characterize inflow, and 15 to characterize the time-varying state of the turbine. For the test, data was sampled at a rate of 40 Hz using the ATLAS II (Accurate GPS Time-Linked Data Acquisition System) data acquisition system. The system features a time-synchronized continuous data stream and telemetered data from the turbine rotor. This paper documents the instruments and infrastructure that have been developed to monitor these blades, turbines and inflow, as well as both modeling and field testing results.

TABLE OF CONTENTS

Page

Abstract 3

TABLE OF CONTENTS 4

LIST OF FIGURES 7

LIST OF TABLES 11

INTRODUCTION 13

TEST SITE 14
- Site Plan 15
- Buildings 15

THE TEST TURBINES 17
- The Micon Turbine 18

INsTRUMENTATION 19
- Instrumentation Summary and Nomenclature 19
- Inflow Instrumentation 21
  - Cup Anemometer 22
  - Wind Vane 22
  - Sonic Anemometers 23
  - Temperature 24
  - Differential Temperature 24
  - Barometric Pressure 24
- Blade Instrumentation 24
  - Strain Gauge Circuits 24
  - Tower Instrumentation 25
  - Nacelle Motion 25
- Additional Instrumentation 25
  - Yaw Position 26
  - Rotor Azimuth and Velocity 26
  - Turbine Status 26
  - Power Production 26

DATA ACQUISITION SYSTEM 27
- ATLAS II 27
- Data Archival 27

Blade Calibration 28
- Calibration Procedure 28
- Calculating Calibration Factors 28

WIRING DIAGRAMS 29
- Instrument Enclosure 29
- Lightning Protection 30

Modeling 31
Background 31
3X-100 Blade Specifications 31
Micon 65 Model 31
Preliminary 3X-100 Performance 32
Bushland Test Site Baseline 33
Linear Region Performance 35
Stall Region Performance 37
Field Data Analysis 39
Background 39
Yaw Drive Problem and Blade Pitch 41
Data Summary 46
Data Analysis 47
Time Series Data Campaign 1 and Campaign 2 47
Power Production 50
Load Spectrum 51
Fatigue Spectra 57
CONCLUDING REMARKS 63
REFERENCES 64
APPENDIX A 65
DETAILED DIAGRAMS OF THE METEOROLOGICAL TOWERS 65
Center Meteorological Tower 66
North, South and Off-Axis Meteorological Towers 67
APPENDIX B 68
INSTRUMENTATION SPECIFICATIONS 68
Met One Instrumentation 68
Cup-and-Vane Anemometry 68
Temperature Measurements 69
Barometric Pressure 70
Sonic Anemometer 70
Strain Gauges 71
Blade Gauges 71
Hub Gauges 72
Tower Bending 72
Accelerations Measurement System 72
Additional Instruments 73
Yaw Position 73
Rotor Azimuth and Velocity 73
Power 74
Control Switch 74
APPENDIX C 75
WIRING DIAGRAMS 75
Instrument Enclosure 75

AC Power Supply 75
DC Power Supplies 75
Lightning Protection 76
Instrument Rack 77
DISTRIBUTION 78

LIST OF FIGURES

Page

Figure 1: Layout Map of the USDA-ARS Site in Bushland, TX. 14

Figure 2: A Schematic Overview of the Test Site. 15

Figure 3: Site Plan with Detailed Dimensions. 16

Figure 4: The Test Turbines at the USDA-ARS Site in Bushland, TX. 17

Figure 5: The Test Turbine. 18

Figure 6: Diagram of the Inflow Instrumentation for the Micon "B" Turbine. 19

Figure 7: Diagram of the Structural Instrumentation for the Micon Turbines. 19

Figure 8: Mounting of the Inflow Instrumentation on an Extension Arm. 22

Figure 9: Tower-Top Mounting of Cup and Vane 23

Figure 10: Mounting of the Temperature and Delta Temperature Probes 23

Figure 11: Rotor Azimuth, Velocity, and Nacelle Yaw Position. 26

Figure 12: 3X-100 Calibration Fixture 28

Figure 13: Instrumentation Rack Located in the Instrument Enclosure. 30

Figure 14: Micon 65 ADAMS Model 32

Figure 15: Power prediction comparison between FAST and ADAMS 32

Figure 16: Predicted Power Curve for the Micon 65 with 3X-100 Blades 33

Figure 17: Simulated Wind Speed Data for a 6 m/s, Turb. B 34

Figure 18: Rotor Power, 6 m/s, Turb. B 34

Figure 19: 3X-100 Flap Bending Moment 35

Figure 20: 3X-100 Edge Bending Moment 35

Figure 21: Simulated Wind Speed Data for a 10 m/s, Turb B. 36

Figure 22: Rotor Power, 10 m/s, Turb. B 36

Figure 23: 3X-100 Flap Bending Moment 37

Figure 24: 3X-100 Edge Bending Moment 37

Figure 25: Simulated Wind Speed Data for a 15 m/s, Turb. B. 38

Figure 26: Rotor Power, 15 m/s, Turb. B 38

Figure 27: 3X-100 Flap Bending Moment 38

Figure 28: 3X-100 Edge Bending Moment 39

Figure 29: Micon Turbine with 3X-100 Blades 40

Figure 30: PSD for Hub Flap 41

Figure 31: Hub flap bending moments. 42

Figure 32: Hub edge bending moments. 42

Figure 33: Calculated oscillatory moment on nacelle 43

Figure 34: Measured 3X-100 initial pitch angles. 44

Figure 35: 3X-100 initial power production. 45

Figure 36: 3X-100 pitch angles after adjustment. 46

Figure 37: Wind Speed Bin Comparison 47

Figure 38: Hub Height Wind Speed 48

Figure 39: Electrical Power 48

Figure 40: Wind Direction 48

Figure 41: Root Flap Bending 48

Figure 42: Root Edge Bending 48

Figure 43: Down Wind Tower Bending 48

Figure 44: Hub Height Wind Speed 49

Figure 45: Electrical Power 49
Figure 46: Wind Direction 49
Figure 47: Root Flap Bending 49
Figure 48: Root Edge Bending 49
Figure 49: Tower Bending 49
Figure 50: Power Production First Campaign 50
Figure 51: Power Production Second Campaign 50
Figure 52: 10-miinute Average Power Production Comparison 51
Figure 53: 10-minute Average First Campaign Hub Edge Bending Moments 51
Figure 54: 10-minute Average Second Campaign Hub Edge Bending Moments 52
Figure 55: 10-minute Average First Campaign Hub Flap Bending Moment 52
Figure 56: 10-minute Average Second Campaign Hub Flap Bending Moment 53
Figure 57: First Campaign PSD for 7 m/s Wind Speed 53
Figure 58: First Campaign PSD for 7 m/s Wind Speed 54
Figure 59: Second Campaign PSD for 7 m/s Wind Speed 55
Figure 60: Second Campaign PSD for 7 m/s Wind Speed 55
Figure 61: First Campaign Azimuth Average Edge and Flap Bending Loads 56
Figure 62: Second Campaign Azimuth Average Edge and Flap Bending Loads 56
Figure 63: First Campaign Azimuth Average Flap Bending Loads 57
Figure 64: Second Campaign Azimuth Average Flap Bending Loads 57
Figure 65: Campaign 1 Edge rainflow count for 7-9 m/s Wind Speeds 58
Figure 66: Campaign 1 Flap rainflow count for 7-9 m/s Wind Speeds 58
Figure 67: Campaign 2 Edge rainflow count for 7-9 m/s Wind Speeds 59

Figure 68: Campaign 2 Flap rainflow count for 7-9 m/s Wind Speeds 59

Figure 69: Comparison of Blade 3 Flap Bending Moments 60

Figure 70: Campaign 1 Edge rainflow count for 9-11 m/s Wind Speeds 60

Figure 71: Campaign 1 Flap rainflow count for 9-11 m/s Wind Speeds 61

Figure 72: Campaign 2 Edge rainflow count for 9-11 m/s Wind Speeds 61

Figure 73: Campaign 2 Flap rainflow count for 9-11 m/s Wind Speeds 62

Figure 74: Comparison of Blade 1 Flap Bending Moments 62

LIST OF TABLES

Page

Table 1: Turbine Instrumentation. 20

Table 2: Turbine Instrumentation. 20

Table 3: Rotor Instrumentation. 21

Table 4: Strain Gauge Circuits. 25

Table 5: 3X-100 Calibration Results 29

Table 6: Blade Weights and Center of Gravity 31

INTRODUCTION

In support of a Work-For-Other (WFO) agreement between the Wind Energy Technology Department at Sandia National Laboratories and 3TEX, one of the three Micon 65/13M wind turbines at the USDA Agriculture Research Service (ARS) center in Bushland, Texas, has been used to test a set of 9 meter wind turbine blades, manufactured by TPI composites using the 3TEX carbon material for the spar cap. Data collected from the test has been analyzed to evaluate both the aerodynamic performance and the structural response from the blades.

For the test, the blade aerodynamic and structural characterization, meteorological inflow, and wind turbine structural response were monitored with a total of 57 instruments: 15 to characterize the blades, 13 to characterize inflow, and 15 to characterize the time-varying state of the turbine. The primary characterization of the inflow relied upon 1 sonic anemometer at hub height, 3 cup anemometers, 2 wind vanes, 2 temperature probes, and 1 barometer. The structural response of the turbine was measured using several sets of strain gauges to measure bending loads on the hubs and towers. To describe the motion of the nacelle, a six-axis inertial measurement unit (IMU) output both acceleration and velocity on all three axes. Data is sampled at a rate of 40 Hz using the ATLAS II (Accurate GPS Time-Linked Data Acquisition System) data acquisition system. The system features a time-synchronized continuous data stream and telemetered data from the turbine rotor.

TEST SITE

The turbine used in this test is located on the USDA-ARS site in Bushland, Texas. This site is characteristic of the Great Plains with essentially flat terrain. The test site is surrounded by farmland. On the NNW corner of the test site is a reservoir surrounded by an approximately 1.2-m (4-ft)-high berm. As illustrated in the map shown in Figure 1, the site slopes down approximately 1 m (3 ft) to the SSE across the span of the turbine bases.

The primary wind direction at the site is from 224° with respect to true north, 215° with respect to magnetic north.† The wind rose for this site shows a secondary peak for winds from approximately due north.

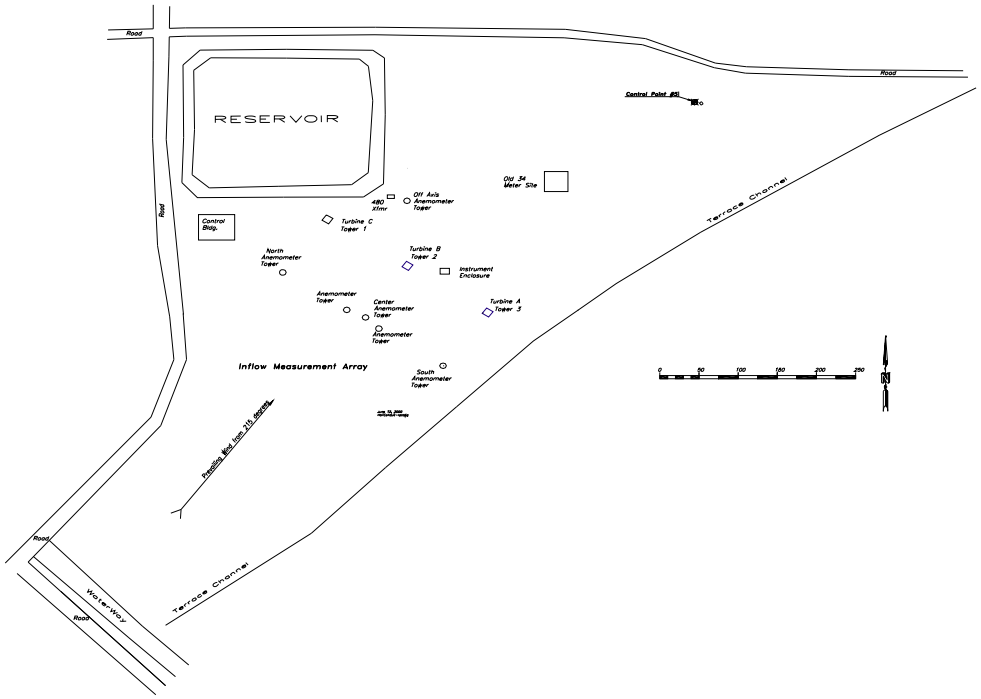

*

Figure 1: Layout Map of the USDA-ARS Site in Bushland, TX.

* * All compass headings are given with respect to Ture North.

Site Plan

As shown in Figure 2, the three turbines have been placed on this site in a straight line across the prevailing wind direction of 215°. The towers are labeled 1, 2, and 3 and the nacelles are labeled A, B, and C.

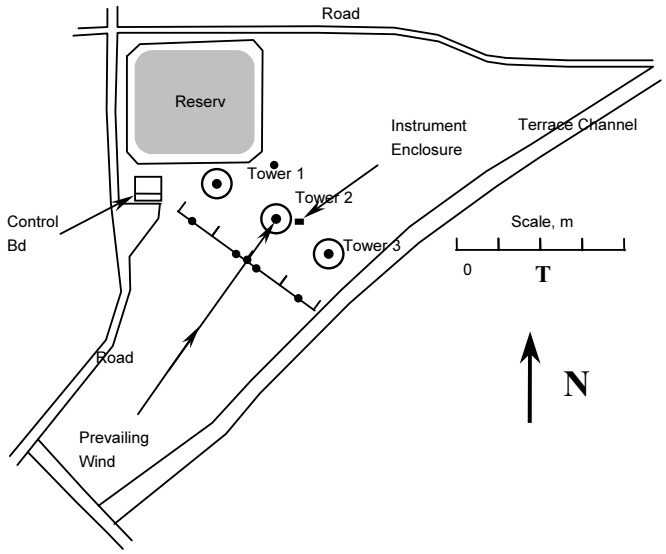

Figure 2: A Schematic Overview of the Test Site.

Upwind of the turbines (with respect to the prevailing winds) are five meteorological (met) towers. As reported previously[1], these towers were equipped with a large array of instrumentation that was used in the previous Long-Term Inflow and Structural Test (LIST) campaign. For the testing of the 3X-100 (3TEX eXperimental - 100kW), only the center met tower was used. For the secondary prevailing wind direction (approximately north) another meteorological tower was used. The nomenclature used to designate each of these towers is given in Figure 3.

A detailed dimensional drawing of the position of the turbines and the meteorological towers is also given in Figure 3 .

Buildings

Two buildings are on the test site (see Figure 2). The main “Control Building” is west of Tower 1. A small ”Instrumentation Building” is located east of Tower 2. The latter building provides environmental protection for a number of signal processors and wiring junction points in the data system. Neither the reservoir nor the buildings obstruct the inflow to the turbines from the prevailing wind direction. For inflow from the secondary wind direction (north), the turbines will also have an unobstructed inflow.

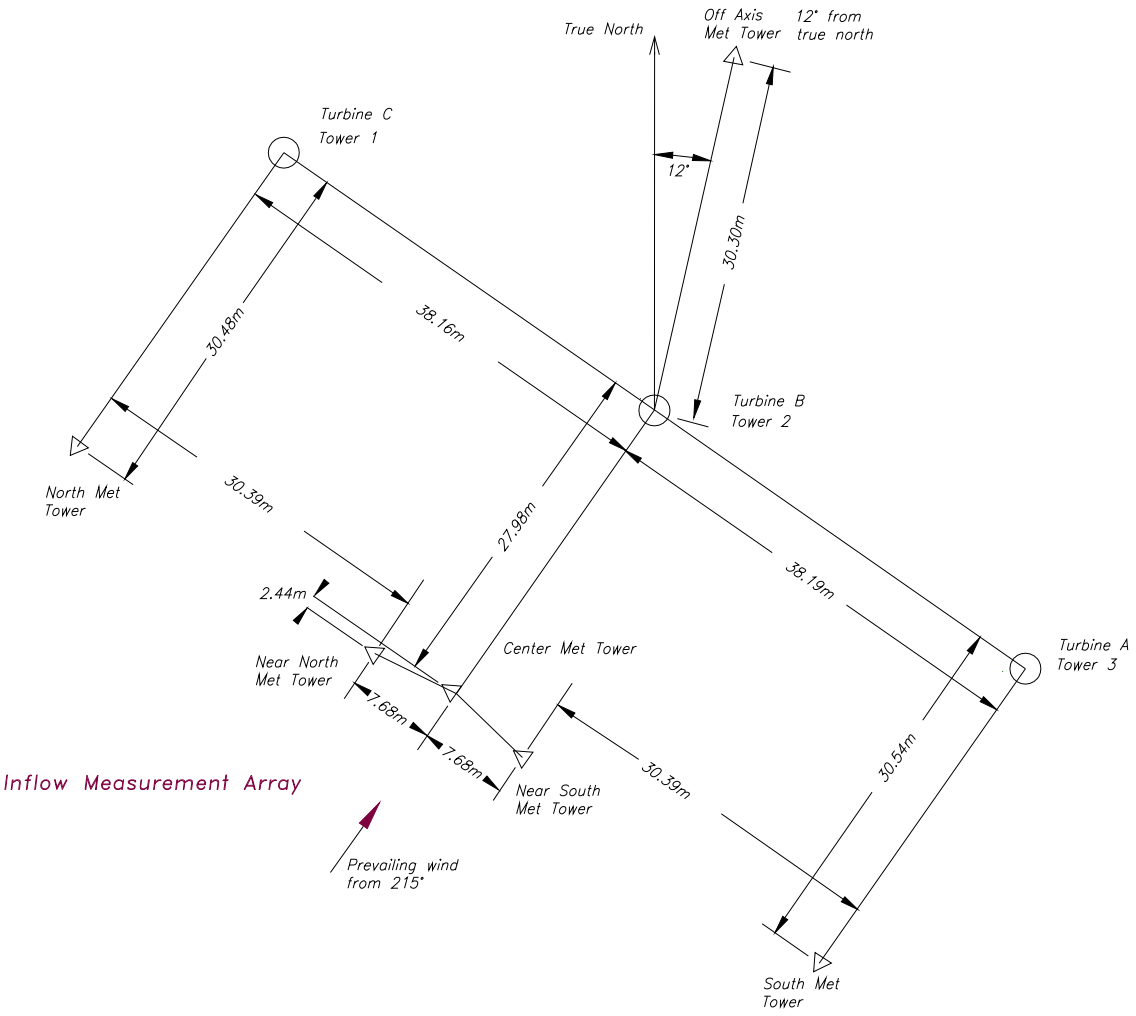

Figure 3: Site Plan with Detailed Dimensions.

THE TEST TURBINES

The turbines are modified versions of the Micon 65/13 turbine (65/13M) (see Figure 4). Each turbine is designed as a three-bladed, fixed-pitch, upwind turbine using an induction generator. At hub height, the turbine stands 23 m (75 ft) tall on a tubular, three-piece steel tower that weighs approximately 64.5 kN (14,500 lb). The nacelle weight is approximately 42.7 kN (9,600 lb).

The turbines are retrofitted machines that ran in the Palm Springs (CA) area for approximately 15 years. During that period, several turbine subsystems were modified to increase performance and reliability. Modified subsystems include the brakes, gearbox, generator and blades. The new drive train is built around an induction, three-phase 480v generator rated at 115 kW. The generator operates at 1200 rpm while the blades turn at a nominal 55 rpm (the standard Micon 65/13 turbine rotates at 45 rpm). A detailed description of the placement of the turbines is provided in Figure 3. During the past year, a second retrofit of the machine was conducted. In order to test a series of 9 meter blades, several components have been heavily modified including: new brakes, faster sensors, new safety infrastructure, and new control algorithms.

Figure 4: The Test Turbines at the USDA-ARS Site in Bushland, TX.

Figure 5: The Test Turbine.

The Micon Turbine

The Micon turbine used in this test campaign is the B nacelle on Tower 2 (see Figure 3 and Figure 5). The "B" turbine is fitted with 3X-100 blades that are based on the ERS100 airfoils and platform. They measure 9 m (354.3 in) in length, yielding a rotor diameter of 19.3 m (63.3 ft). The design consists of a fiberglass shell with a carbon fiber sparcap manufactured using the 3TEX 3D Woven material. The hub flange for mounting the blades is located 599 mm (23.6 in) from the centerline of the low-speed shaft. The hub is a fixed-pitch blade design. The blades are designed to have 0° pitch at the 95 percent span line.

INSTRUMENTATION

The turbine and the meteorological inflow at the Bushland test site were being monitored with a total of 57 instruments: 15 to characterize the blades, 13 to characterize inflow, and 15 to characterize the time-varying state of the turbine. Primary structural characterization of the blade response consisted of 9 sets of strain gauges for the 3X-100 to measure bending loads on the blades, and 8 instruments to measure the tower and nacelle motion. Most of the instrumentation was concentrated on the inflow towers and the test turbine. See the schematic diagrams shown in Figure 7 and Figure 6 for details.

Instrumentation Summary and Nomenclature

A complete list of the 57 instruments used here is presented in Tables 1, 2 and 3. These tables divide the instruments into three general classifications: inflow, rotor, and nacelle. The nomenclature used to identify each gauge circuit is also included in these tables.

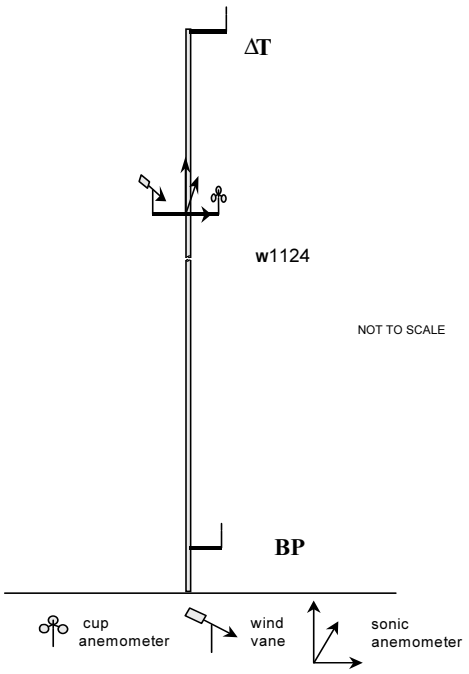

Figure 7: Diagram of the Inflow Instrumentation for the Micon "B" Turbine.

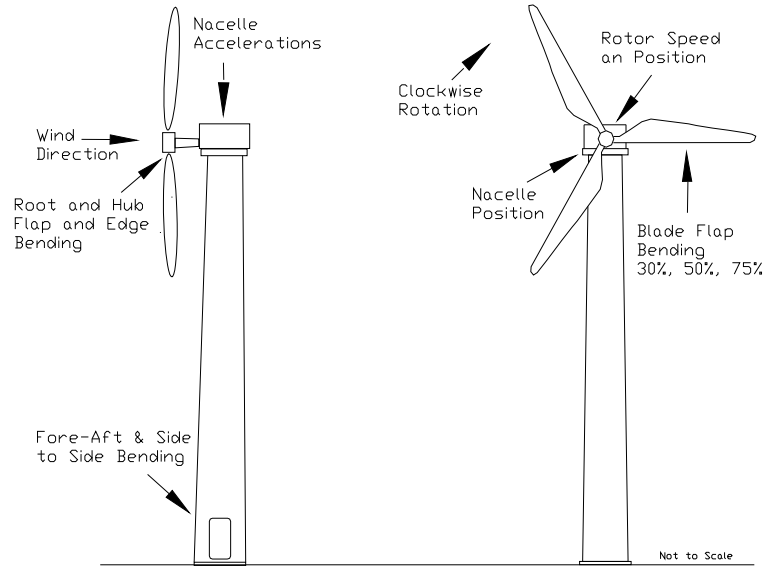

Figure 6: Diagram of the Structural Instrumentation for the Micon Turbines.

Table 1: Turbine Instrumentation.

Name	Instrument	Location	Placement
BAHHATIU	Ultrasonic Anemometer	Center Met Tower	Hub Height
BAHHATIV			
BAHHATIW			
BAHHATIT			
BAHHC	Cup		
BAHHV	Wind Vane		
BATP	Temperature		2m
BADTP	Differential Temperature		Hub Height
OHHC	Cup	Off-Axis Met Tower	
OHHV	Wind Vane		
EPR	Barometric Pressure	Instrument Building	2m
BA2mC	Cup	Center Met Tower	3m

Table 2: Turbine Instrumentation.

Name	Instrument	Location	Placement
3TEXFA	Tower Bending	Tower	12 Feet
3TEXSS			
3TEXOO	Turbine Monitor	Tower Base	
3TEXP	Turbine Power		
SERI_TP	Neighbor Turbine Power	Tower Base	
PLC_BRAKE	Brake Monitor Circuit		
3TEXYAW	Yaw Position	Nacelle	
3TEXRA	Rotor Azimuth		
3TEXRS	Rotor Speed		
3TEXAX	Fore-Aft Acceleration		
3TEXAY	Side-to-Side Acceleration		
3TEXAZ	Up-Down Acceleration		
3TEXRX	Pitch Rate		
3TEXRY	Roll Rate		
3TEXRZ	Yaw Rate		

Table 3: Rotor Instrumentation.

Name	Instrument	Location	Placement
3TEXB1RF	Root Flap Bending	Blade 1	Rotor
3TEXB1RE	Root Edge Bending		
3TEXB12250	Flap Bending - 2550 mm		
3TEXB14500	Flap Bending - 4500 mm		
3TEXB16750	Flap Bending - 6750 mm		
3TEXB1HF	Hub Flap Bending		
3TEXB1HE	Hub Edge Bending		
3TEXB2RF	Root Flap Bending	Blade 2	
3TEXB2RE	Root Edge Bending		
3TEXB2HF	Hub Flap Bending		
3TEXB2HE	Hub Edge Bending		
3TEXB3RF	Root Flap Bending	Blade 3	
3TEXB3RE	Root Edge Bending		
3TEXB3HF	Hub Flap Bending		
3TEXB3HE	Hub Edge Bending		

Inflow Instrumentation

The meteorological inflow for the test turbine was monitored with cup anemometers, wind vanes, and a sonic anemometer (see Figure 7). As noted above, this instrumentation was mounted on two meteorological towers. Figure 3 provides a detailed description of the position of each meteorological tower and its nomenclature. Appendix A provides a detailed diagram of each tower.

Most of the anemometry was located at approximately 30.7 m (101 ft) upwind (with respect to the prevailing wind) of the turbines. This dimension is equivalent to approximately 1.6 rotor diameters in front of the turbines.

There were three towers directly in front of the tower 2 “B” Nacelle (see Figure 3). The center tower was directly upwind (with respect to the prevailing wind) of the test turbine. The other two towers were used on previous tests, and were not used for the 3X-100 test. The center meteorological tower had one cup anemometer, a wind vane, and a sonic anemometer mounted at hub height (see Figure 7). To monitor the secondary wind direction, a cup anemometer and a wind vane were mounted at hub height on the off-axis met tower that is located at approximately 30.3 m directly north of Tower 2 (see Figure 3).

The inflow instrumentation on the center meteorological tower was mounted on the end of an extension arm to preclude blockage effects from the tower (see Figure 8). This extension or boom arm held the instrumentation approximately 2.4 m (7.9 ft) in front of the meteorological tower, with respect to the primary prevailing winds. This is equivalent to 5 anemometer tower diameters. The arm was mounted in a roller support housing that permits the instrumentation to be rolled towards the tower for maintenance. The arm was stabilized vertically and horizontally with two supporting brackets. The center tower was set back to compensate for the extension provided by this boom (see Figure 3) to place all of the anemometry in the same plane perpendicular to the prevailing winds. The inflow instrumentation on the other tower was mounted on the top of the tower, and therefore no extension arms were required (see Figure 9 for a diagram of a typical installation).

Cup Anemometer

Three cup anemometers were used to monitor the inflow. Two were placed at hub height, one in front (with respect to the primary prevailing winds) of the test turbine and another at hub height in the secondary wind direction (see Figure 7). The third cup was on the center met tower two meters from ground level.

The cup anemometer was a Wind Speed Transmitter (cup), Model 1564B, provided by Met One Instruments Incorporated.[2] A complete description of this instrument is provided in Appendix B. The mounting method is shown in Figure 8.

Wind Vane

A total of two wind vanes were used in this installation and all were placed at hub height. One was placed in front of the test turbine (with respect to the primary prevailing winds), and the second was placed at hub height in the secondary wind direction.

The wind vane installations are shown in Figure 8. The system used is a Wind Direction Transmitter, Model 1565C, provided by Met One Instruments Incorporated[2] (see Appendix B).

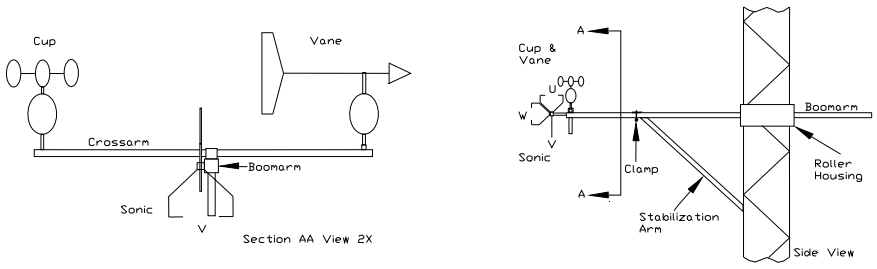

(a) Front View. **(b) Side View.**

Figure 8: Mounting of the Inflow Instrumentation on an Extension Arm.

Sonic Anemometers

One sonic anemometer was used in this installation positioned in front (with respect to the primary prevailing winds) of Tower 2. The location of this anemometer on the tower is shown in Figure 3.

The sonic anemometer installation is shown in Figure 8. The system was a model SATI/3K, Applied Technologies Incorporated[3] (see Appendix B). The unit measures three velocity components and the "sonic" temperature (calculated from the wind speed). The positive wind direction for the U component was 215°, the positive wind direction for the V component was 125°, and the positive wind direction for the W component is vertically up.

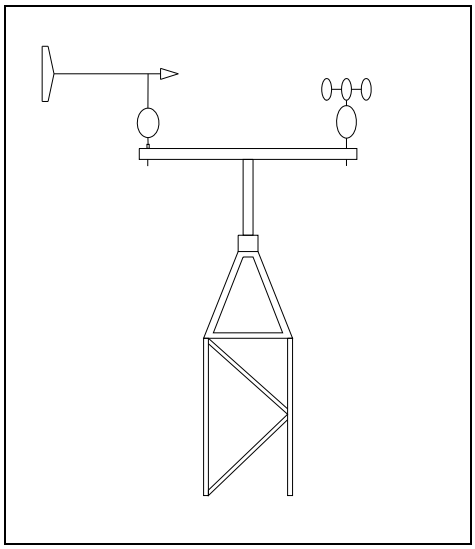

Figure 9: Tower-Top Mounting of Cup and Vane

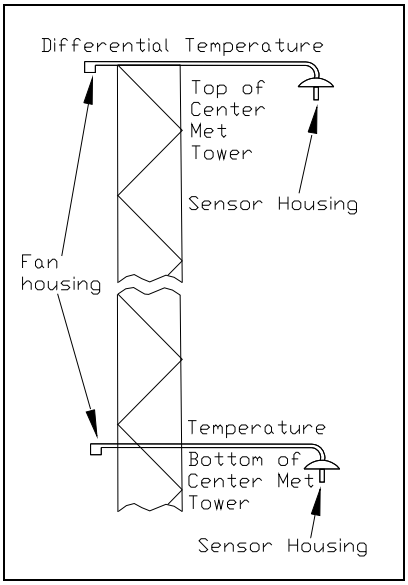

Figure 10: Mounting of the Temperature and Delta Temperature Probes

Temperature

The absolute temperature was measured at the center meteorological tower, approximately 1.6 m (5.1 ft) above ground level, by a four-wire platinum resistance temperature (PRT) detector, Met One Model No. 0631.[2] The temperature sensor was mounted with a solar shield on the end of a tubular arm at about 1 m from the tower in the prevailing wind direction of 215° (see Figure 10 and Appendix B).

Differential Temperature

The differential temperature was measured on the center meteorological tower, between the top of the tower at 33.6 m (110 ft) and at ground level 1.6 m (5.1 ft) by a four-wire platinum resistance temperature (PRT) detector (the absolute temperature discussed above). A positive differential temperature reading indicates that the temperature at the top of the rotor is higher than the temperature at ground level.

Barometric Pressure

The absolute barometric pressure was measured at approximately 2.13 m (7 ft) above ground level, inside the Instrument Building (see Appendix B), using a sensor manufactured by Yellow Spring Instruments.[4]

Blade Instrumentation

The structural response of the blades on the rotor was measured with a variety of gauges, primarily strain gauges. A schematic of the strain measurement locations is shown in Figure 6.

Most of the strain gauge circuits were placed on the rotor. Each blade was instrumented at its root, and one blade was instrumented at approximately 25, 50, and 75 percent span station with strain gauge bridges that measured flap bending. Upon installation, all strain gauges were verified and calibrated by statically loading the blade.

Strain Gauge Circuits

A total of 15 strain gauge circuits were used for the 3X-100 blade test (see Figure 6). A complete list of the strain gauge circuits is given in Table 4. A full bridge completion unit was used on all circuits.

Blade Strain Gauges

The strain gauges were dual–element, encapsulated 350-ohm gauges (Micro Measurements WK-06-250PD-350)[5] located at the root, 25, 50, and 75 percent of span of one blade and only at the root on the other two blades (see Figure 6 and Appendix B).

Hub Strain Gauges

The strain gauges were dual–element, encapsulated 350-ohm gauges (Micro Measurements WK-06-250PD-350)[5] located on each arm of the hub (see Figure 6 and Appendix B).

Table 4: Strain Gauge Circuits.

Type	Active Elements	Position	Gauge Type	Resistance (ohms)	DAS Channel	Direction
Bending	2	Tower	WK-06-250TM-350	350	3TEXFA	Fore-Aft
					3TEX SS	Side-to-Side
	4	Hub 1	WK-06-250PD-350	350	3TEXHF	Hub Flap
					3TEXB1H	Hub Edge
		Blade 1	WK-06-250PD-350	350	3TEXB1RF	Root Flap
					3TEXB1RE	Root Edge
					3TEXB12250	25 % Flap
					3TEXB14500	50 % Flap
					3TEXB16750	75 % Flap
		Hub 2	WK-06-250PD-350	350	3TEXB2HF	Hub Flap
					3TEXB2HE	Hub Edge
		Blade 2	WK-06-250PD-350	350	3TEXB2RF	Root Flap
					3TEXB2RE	Root Edge
		Hub 3	WK-06-250PD-350	350	3TEXB3HF	Hub Flap
					3TEXB3HE	Hub Edge
		Blade 3	WK-06-250PD-350	350	3TEXB3RF	Root Flap
					3TEXB3RE	Root Edge

Tower Instrumentation

The tower was instrumented with dual-element, encapsulated 90° tee rosette, 350-ohm gauges. These bending circuits use Micro Measurements WK-06-250TM-350 strain gauges[5] (see Figure 6 and Appendix B). The gauges are located approximately 3.9 m (154 in) above the turbine base. One set measures tower fore-aft bending (along the prevailing wind direction) and the other measures side-to-side bending (across the prevailing wind direction).

Nacelle Motion

The nacelle was instrumented with one Micro-Electro-Mechanical Systems (MEMS) device six-axis inertial measurement unit (IMU). The IMU measured the fore-aft, side-to-side, and up-down accelerations with three MEMS accelerometers, as well as pitch, roll, and yaw rates with three angular rate sensors consisting of vibrating ceramic plates that utilize the Coriolis force to output angular rate independent of acceleration. The instrument was a Crossbow Inertial Measurement Unit, IMU300CC-100,[6] located on the nacelle frame next to the gearbox (see Figure 6 and Appendix B).

Additional Instrumentation

In addition to the instrumentation cited above, several other turbine parameters were measured (see Table 2). These include nacelle yaw position, rotor position, rotor speed, turbine monitor (on-off switch), and electrical power output. The yaw and rotor positions were measured directly with 360° angle encoders. The turbine monitor indicated the state of the grid and turbine connection, i.e., whether or not the turbine was connected to the grid. The electrical power production for the test turbine was monitored using a three-phase electrical power transducer.

Yaw Position

Nacelle yaw position was measured using a brushless rotary encoder, Computer Conversions Corporation model HSTDCC-PB16S-SE.[7] The encoder was located on the yaw drive gear box inside the nacelle (see Figure 11). The encoder shaft was connected to the yaw drive using a toothed belt pulley system. The sizes of the pulleys in this system were chosen to yield a 1:1 rotation ratio between the encoder and the yaw position (see Appendix B). The unit was calibrated to yield a yaw measurement of zero when the nacelle points to true north.

Rotor Azimuth and Velocity

Rotor azimuth and velocity were measured by a brushless rotary encoder (Model No. EVSTDCC-PB16VIC-SIRPS from Computer Conversions Corporation[7]). The encoder was located adjacent to the low speed shaft on the nacelle (see Figure 11). The encoder shaft was connected to the main drive shaft using a sprocket-chain drive gear system. The sizes of the gears in this system were chosen to yield a 1:1 rotation ratio between the encoder and the main shaft (see Appendix B). The unit was calibrated to yield a 0° signal output when Blade 1 is vertically up. The blade numbering sequence for the rotor is 1-3-2 clockwise as observed from the upwind direction.

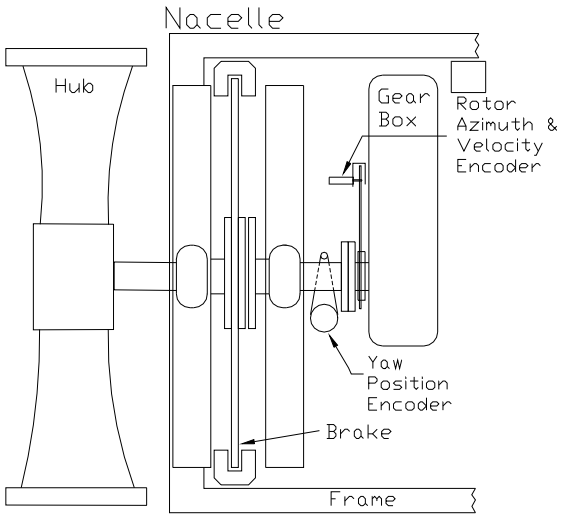

Figure 11: Rotor Azimuth, Velocity, and Nacelle Yaw Position.

Turbine Status

The turbine monitor circuit was an on/off signal that indicated if the turbine was connected to the grid; i.e., the turbine rotor rpm was up to speed and the generator was connected to the utility grid. This signal was derived from the controller signal that engages the generator-to-grid connection; an auxiliary power supply, driven by the control signal, was used to supply the on/off voltage signal to the data acquisition system. The relay, in the controller, was located in the turbine control junction box at the base of the turbine tower.

Power Production

The electrical power produced by each of the three turbines was monitored using precision self-powered voltage, current watt, volts amps reactive (VAR), and transducers from Ohio Semitronics.[8] For this installation, only the total power (three-phase) was recorded. As warranted, additional electrical measurements may or may not be added to the data record. The electrical instruments were located in the turbine control junction boxes at the base of each turbine tower (see Appendix B.)

DATA ACQUISITION SYSTEM

For the test, the Accurate GPS Time-Linked Data Acquisition System[1,9] (ATLAS II) was used. The ATLAS II is designed to acquire long-term, continuous, time-synchronized, multi-channel time series data from meteorological towers and an operating wind turbine. The 16-bit data stream from the ATLAS II hardware system was acquired and recorded using the ATLAS II software. The software segments the continuous data stream into 10-minute blocks and stores them for future processing. The data can be stored in raw state as the data is collected or it can be converted to engineering units using calibration factors.

For this series of experiments, the data sample rate was 40 Hz. This yields a Nyquist frequency of 20 Hz, which was sufficient for capturing the behavior of the inflow and the structural response of the turbine.

ATLAS II

For this experiment, two ATLAS II boxes were used in the data acquisition system (DAS). The first ATLAS II unit was a ground-based unit (GBU). This unit was located in the Instrument Enclosure near the base of Tower 2 (see Figure 2). The second was a rotor-based unit (RBU) that was mounted to the rotor.

The GBU was mounted in the "instrumentation rack" inside the instrument enclosure (see Appendix C). It monitored the instrument circuits cited in Table 1 and Table 2; i.e., all instruments except the strain gauge circuits on the rotors. The GBU had five 8-channel analog cards and one 8-channel bridge card. The bridge and analog circuits used a second-order anti-aliasing active filter followed by a programmable fifth-order Butterworth filter. The cut-off frequency for the latter filter was set to 20 Hz, the Nyquist frequency.

The rotor strain gauges were monitored with the RBU. This unit, called "Windy," contained three 8-channel bridge circuit cards that monitored the strain gauge circuits described in Table 3. Data from the RBU is telemetered to the computer. The computer integrated the GBU and RBU data streams to form a single data stream.

A total of 57 channels (timing, measurement, and synchronizing channels) are monitored with this system computer.

All of these units (GBU and RBU) are programmed using an ATLAS II software package developed by Zayas, Ortiz-Moyet and Jones.[1] The GBU can be programmed via a fiber-optic link, while the RBU is currently programmed through a hardwired connection.

Data Archival

The ATLAS II system PC was networked to a data archival and processing PC, also located in the Control Building. This data archival PC retrieved the data from the acquisition PC and performed a series of verifications to ensure data integrity in addition to calculating simple statistics on the data. This allowed the data to be verified, ensuring that all channels are working.

Approximately once a week the site test engineer downloaded the zipped data files to DVD for permanent storage and analysis. When the download was complete, the archived files were removed from the hard disk to free space for the next set of data files.

BLADE CALIBRATION

Calibration Procedure

All three blades were calibrated before the machine was installed on its tower both in flap and edge. The blades were individually mounted onto a calibration fixture in the assembly building in Bushland. Once mounted, data was collected at every load increase in flap and edge. Each blade was pulled to 350 lb in 50 lb increments at a distance of 7.4 meters from the blade flange and the load was monitored using a calibrated load cell (see Figure 12

Figure 12: 3X-100 Calibration Fixture

Calculating Calibration Factors

During the calibration of all three blades the data collected was processed in order to calculate the calibration factors for each blade. An Excel spreadsheet developed at SNL was used to calculate all of the bending moments from the blade pulls and generate a list of calibration factors. These factors are important in order to convert the data from counts, which is the values output from the hardware, into something more meaningful. For the processed data collected all strain measurements are recorded in kN-m, which is a standard unit in the wind energy community (see Table 5).

Table 5: 3X-100 Calibration Results

3X-100-Flap - Blade 1													
Pull Force (lb):		0	50	103	145	194	247	299	353	253	147	53	
Force (kN):		0	0.2224111	0.4581669	0.6449922	0.8629551	1.0987108	1.3300184	1.5702224	1.1254	0.653889	0.235756	
Moment @ SG (kN-m):	Distance to SG												**Slope**
Moment Arm (m) - Hub:	7.5946	0	1.68912334	3.4795941	4.8984577	6.5537986	8.3442693	10.100958	11.925211	8.546964	4.966023	1.790471	0.008053
Moment Arm (m) - Root:	7.041	0	1.56599656	3.2259529	4.54139	6.0760666	7.736023	9.3646594	11.055936	7.923943	4.60403	1.659956	0.004101
Moment Arm (m) - Flap (2.55):	4.841	0	1.07669214	2.2179858	3.1224072	4.1775655	5.3188591	6.438619	7.6014465	5.448062	3.165475	1.141294	0.012463
Moment Arm (m) - Flap (4.50):	2.891	0	0.64299049	1.3245604	1.8646724	2.4948031	3.176373	3.8450831	4.5395129	3.253532	1.890392	0.68157	0.010052
Moment Arm (m) - Flap (6.75):	0.641	0	0.14256552	0.293685	0.41344	0.5531542	0.7042736	0.8525418	1.0065125	0.721382	0.419143	0.151119	0.0014
Cal Data	7.5946	35970	36200	36410	36580	36790	37020	37240	37460	37030	36590	36210	
	7.041	30140	30570	30960	31280	31670	32070	32450	32860	32120	31320	30610	
	4.841	35150	35210	35330	35380	35460	35540	35660	35740	35530	35350	35190	
	2.891	36600	36560	36610	36660	36700	36800	36880	37000	36820	36700	36610	
	0.641	34530	34530	34680	34730	34790	34950	35050	35210	34890	34710	34530	
3X-100-Flap - Blade 2													
Pull Force (lb):		0	50	103	144	201	252	295	353	246	149	49	
Force (kN):		0	0.2224111	0.4581669	0.640544	0.8940926	1.1209519	1.3122255	1.5702224	1.094263	0.662785	0.217963	
Moment @ SG (kN-m):	Distance to SG												**Slope**
Moment Arm (m) - Hub:	7.5946	0	1.68912334	3.4795941	4.8646752	6.7902758	8.5131816	9.9658277	11.925211	8.310487	5.033588	1.655341	0.00794
Moment Arm (m) - Root:	7.041	0	1.56599656	3.2259529	4.5100701	6.2953062	7.8926226	9.2393797	11.055936	7.704703	4.66667	1.534677	0.003988
Cal Data	7.5946	35040	35250	35470	35650	35890	36100	36300	36540	36090	35680	35250	
	7.041	32390	32790	33200	33540	33980	34380	34720	35170	34370	33600	32830	
3X-100-Flap - Blade 3													
Pull Force (lb):		0	49	96	148	203	250	296	344	246	153	52	
Force (kN):		0	0.21796288	0.4270293	0.6583369	0.9029891	1.1120555	1.3166737	1.5301884	1.094263	0.680578	0.231308	
Moment @ SG (kN-m):	Distance to SG												**Slope**
Moment Arm (m) - Hub:	7.5946	0	1.65534087	3.2431168	4.9998051	6.8578408	8.4456167	9.9996102	11.621169	8.310487	5.168717	1.756688	0.007804
Moment Arm (m) - Root:	7.041	0	1.53467662	3.0067134	4.6353498	6.357946	7.8299828	9.2706996	10.774056	7.704703	4.791949	1.628636	0.004403
Cal Data	7.5946	30520	30740	30940	31170	31390	31600	31800	32020	31580	31190	30740	
	7.041	33490	33840	34170	34560	34930	35270	35600	35950	35280	34630	33910	

WIRING DIAGRAMS

The 57 instrument channels that were monitored in this measurement campaign were hardwired to the two ATLAS II units. The myriad of cables and junction boxes that were required to power and monitor the instrumentation are described here. Appendix C presents a complete set of the wiring diagrams for each cable bundle and junction box.

Instrument Enclosure

The large number of wires, "black boxes," power supplies, lightning protection, terminal strips, and telemetry signals were housed in the instrument enclosure (see Figure 13). This enclosure was sealed to protect the instruments from rain, dust, rodents, etc. Most of the hardwired circuits into and out of the enclosure had lightning protection. The instrument enclosure was a large electrical junction box 1.83 m (6 ft) wide by 1.83 m (6 ft) high by 0.61 m (2 ft) deep with circulation fans for cooling and environmental seals around its doors.

The enclosure was located in a small metal shed near the base of Tower 2 (see Figure 2). The shed is heated and cooled by a wall-mounted heat pump.

The enclosure was divided into two primary sections. The southwest side contained a slide-out instrument rack for mounting the data system and associated converters (signal processors) and power supplies. The rack was mounted on slides to permit the rack to be pulled out for easy access to front and rear control panels and wiring connections. The northeast side of the building contained connection boards and the lightning protection.

The enclosure also housed auxiliary power supplies and the uninterruptible power supply (UPS) unit that supplied AC power to all of the instrumentation and data systems.

The instrument rack, instrument enclosure, and the instrument building was grounded through a grid that is connected to the turbine towers, meteorological towers, guy wires, and test site buildings (see Appendix D).

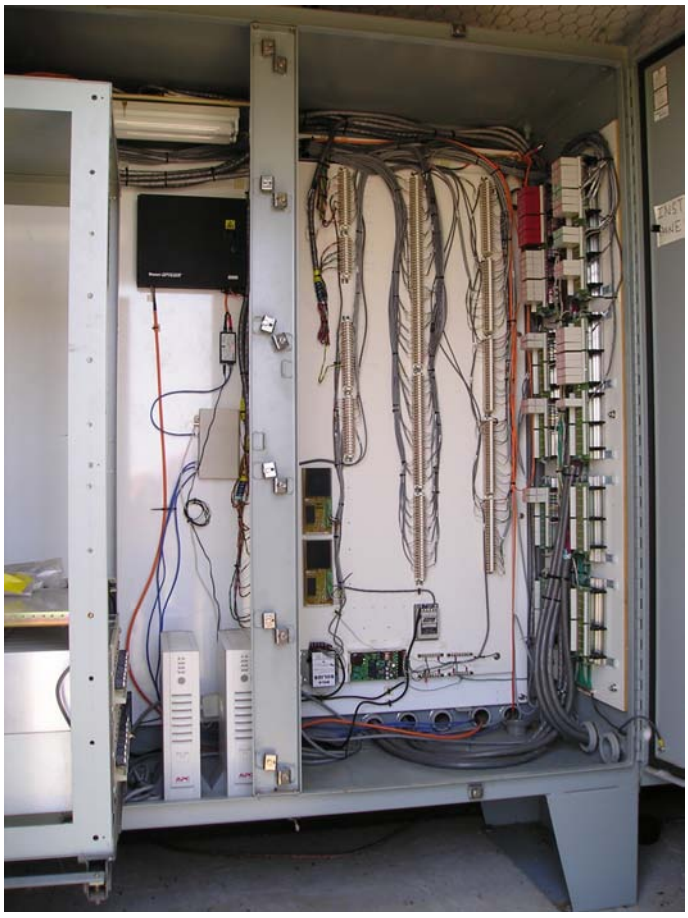

Figure 13: Instrumentation Rack Located in the Instrument Enclosure.

Lightning Protection

Because the Bushland test site is often subject to severe lightning storms, careful attention was paid to protecting the system from lightning damage. The first line of defense was the placement of an extensive ground grid that circles the site and each piece of equipment (see Appendix D). All instrument and circuit grounds and cable shields were connected to this ground grid.

Almost all of the electrical instrumentation leads into and out of the enclosure were protected with commercial high-speed gas tube/avalanche diode lightning protection circuits (Citel Inc.).[11] The specifications for these circuits are in Appendix C. The only circuit without lightning protection was a low-power data reception antenna lead connected to the data collection PC.

The ATLAS II units were connected to the main PC via fiber optics. This eliminated the susceptibility to lightning damage by isolating the instruments inside the instrument enclosure from the computers in the control room. Fiber optics units manufactured by Fiberplex[12] were used.

All circuits in the data acquisition system on the rotor were also protected using commercial high-speed gas tube/avalanche diode lightning protection circuits (Citel Inc.).

MODELING

Background

In order to study the performance of the 3X-100 blades, simulations were conducted using the MSC/ADAMS and the FAST codes [14-16]. ADAMS is a flexible, multi-body dynamic simulation software with virtually unlimited degrees of freedom. The FAST code was originally developed at Oregon State but has been extensively modified by National Renewable Energy Laboratory (NREL) [14]. As with Garrad Hassan's code Bladed, FAST uses a modal representation to model both the blades and the tower. For the aerodynamic loads, FAST and ADAMS utilize the AeroDyn aerodynamic subroutines to generate the blade loads. The FAST code uses a series of text input files that allow the user to relatively quickly generate a wind turbine model, which can be quite complicated to do in ADAMS, since it is a general purpose dynamics code.

3X-100 Blade Specifications

The 3X-100 blades were mounted to the turbine with custom steel mounting in order to compensate for the difference in the mounting bolt pattern of the blades and the hub flange. The blades were weighed with and without the mounting plates and the center of gravity for each blade was also measured. The results are shown in Table 6 .

Table 6: Blade Weights and Center of Gravity

Weight (lb)	Hub 1 blade	Hub 2 blade	Hub 3 blade
w/o plate	387	394	389
w/ mounting plate	543	543	544
CG (distance from plate, in)			
w/o plate	94	95.25	94.75
w/ mounting plate	67	69	69

Micon 65 Model

For the analysis of the 3X-100 blades, the SNL model of the Micon 65 wind turbine was used (Figure 14). The model has been used quite heavily for the latest modifications to the machine and has performed quite well. The model incorporates all of the modifications that have been performed through the years on the test turbine, including the more recent improvements. Most of the calculations on the 3X-100 blades were performed using the FAST code, and periodically were crosschecked with the ADAMS code. The baseline results from both the FAST and the ADAMS models were compared periodically to each other to ensure that the model was accurate. As can be seen in Figure 15, the results from the two codes are quite similar.

Figure 14: Micon 65 ADAMS Model

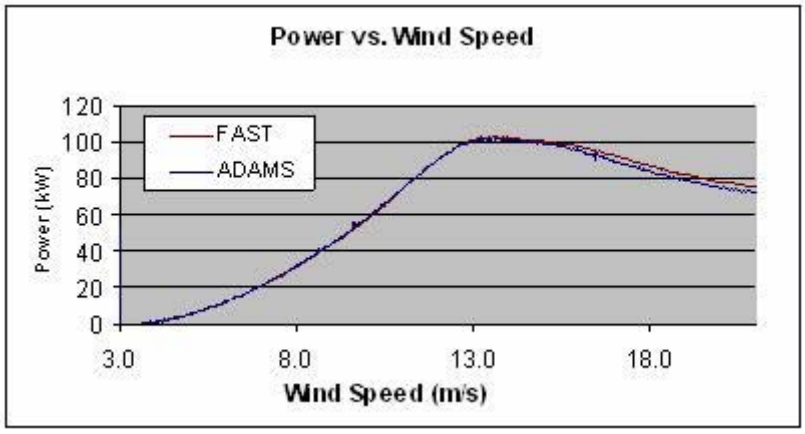

Figure 15: Power prediction comparison between FAST and ADAMS

Preliminary 3X-100 Performance

In order to understand the performance of the 3X-100 blades, a simulation was done where a steadily increasing wind input file was used. This was done to characterize both the power output and the root bending moments in flap and edge. The Micon 65 was originally a 65 kW turbine, but prior to the purchase in 2000, both the gearbox and the generator had been replaced with 115kW units. Even though the rotor diameter has increased by ~3 meters the power output of the machine is still within the limits of both the gearbox and the generator, as shown in Figure 16. At the time the calculations were performed, no data had been collected from the machine, so the results from the model have not been validated. There is, on the other hand, vast data from the previous campaign, where the machine flew with the SERI blades and power outputs of over 120kW were not uncommon. Although the SERI blades are ~1 meter shorter in length, the blades had a much higher solidity.

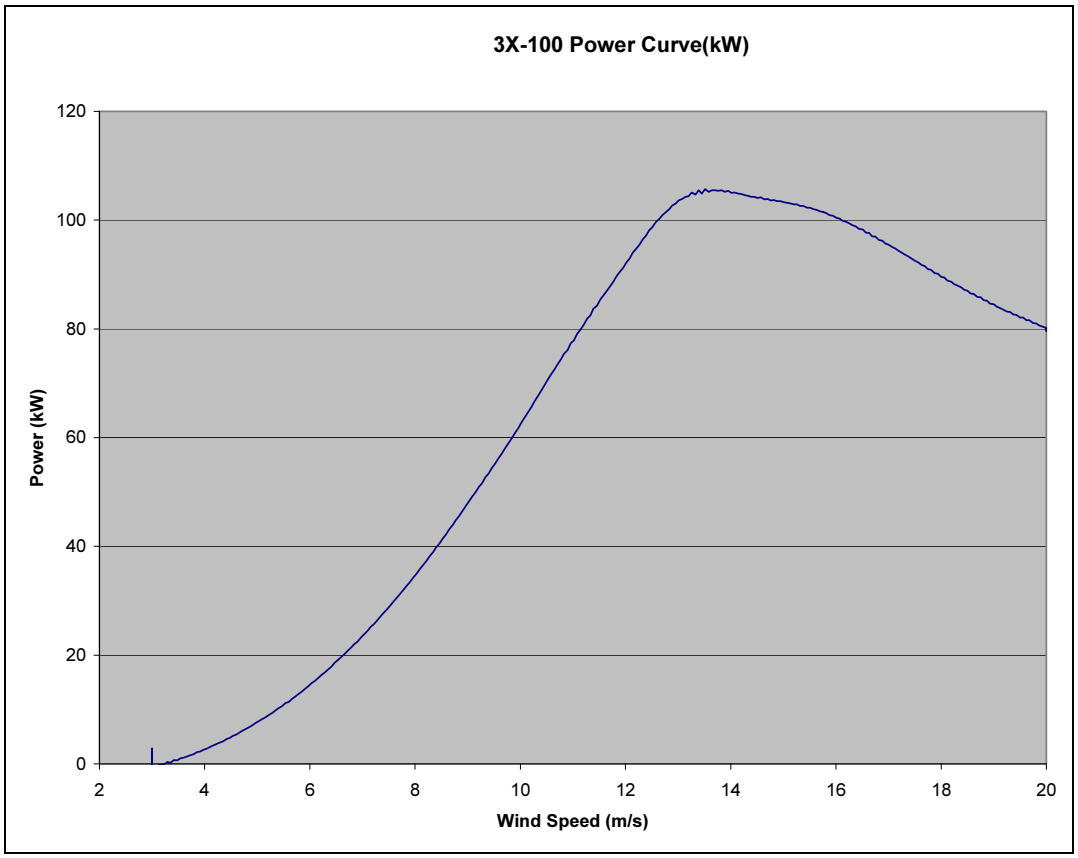

Figure 16: Predicted Power Curve for the Micon 65 with 3X-100 Blades

Bushland Test Site Baseline

The Bushland test site has an annual wind speed of ~6 m/s, and falls under a class 4 wind site according to the IEC standards. The turbulence intensity is "B", according to IEC standards, which is considered a medium level of turbulence of approximately 14%. Figure 19 and Figure 20 show the loads for both the flap and edge root bending moment for the Micon 65 operating in a Class 4-turbulence B wind input file. The power produced is shown in Figure 16. All of the results are using the 3X-100 blades at a 0° pitch setting.

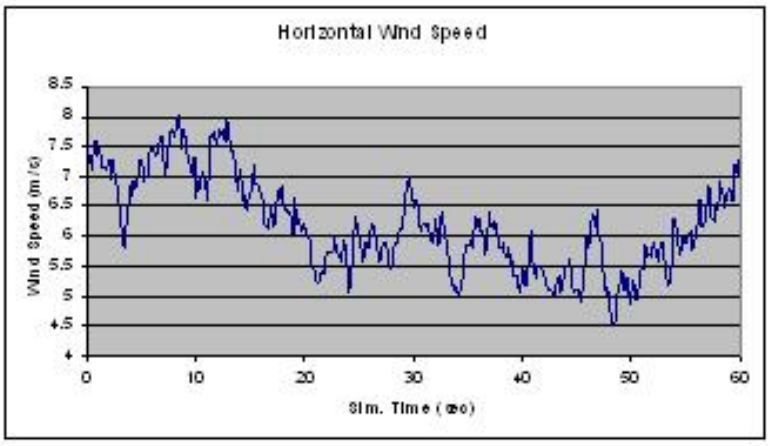

Figure 17: Simulated Wind Speed Data for a 6 m/s, Turb. B

Figure 18: Rotor Power, 6 m/s, Turb. B

For the Class 4-turbulence B file, the root bending moments in flap and edge are plotted in Figure 19 and Figure 20.

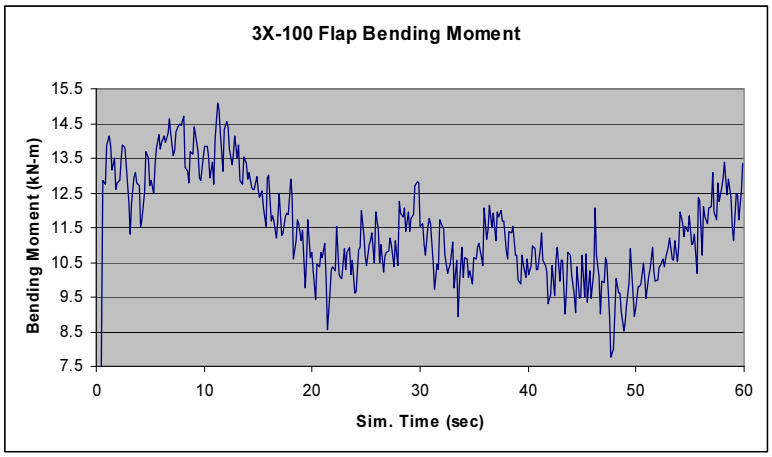

Figure 19: 3X-100 Flap Bending Moment

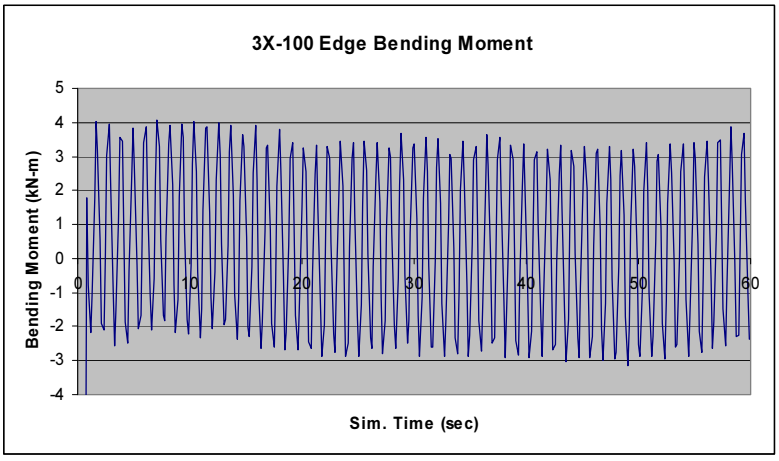

Figure 20: 3X-100 Edge Bending Moment

Linear Region Performance

As can be seen from the simulated power curve in Figure 16, the linear portion of the power curve starts approximately at 7 m/s and ends at 13 m/s. In order to quantify the performance in this region, a 10 m/s, turbulence intensity "B" has been simulated. Figure 21 and Figure 22 show the simulated wind file and the power produced. The root bending moments can be seen in Figure 23 and Figure 24.

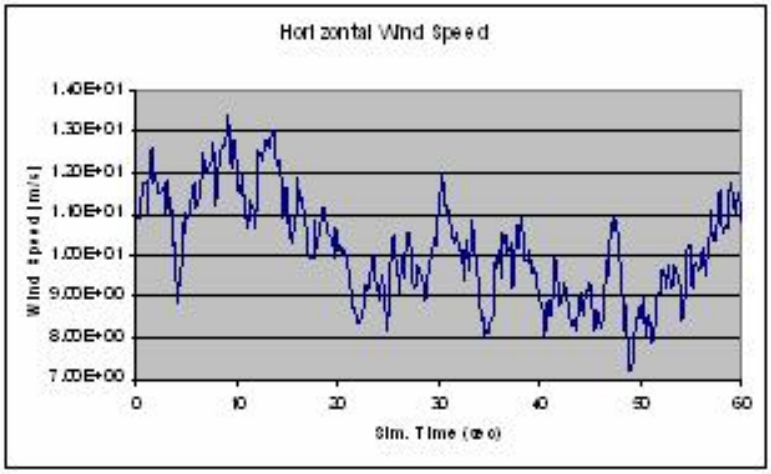

Figure 21: Simulated Wind Speed Data for a 10 m/s, Turb B.

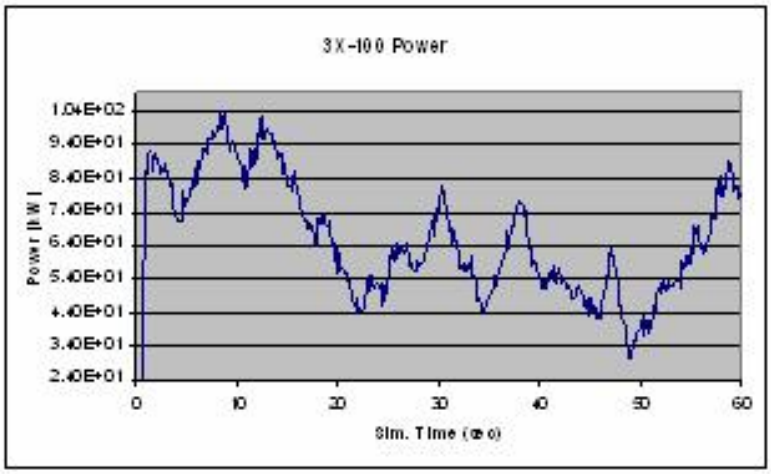

Figure 22: Rotor Power, 10 m/s, Turb. B

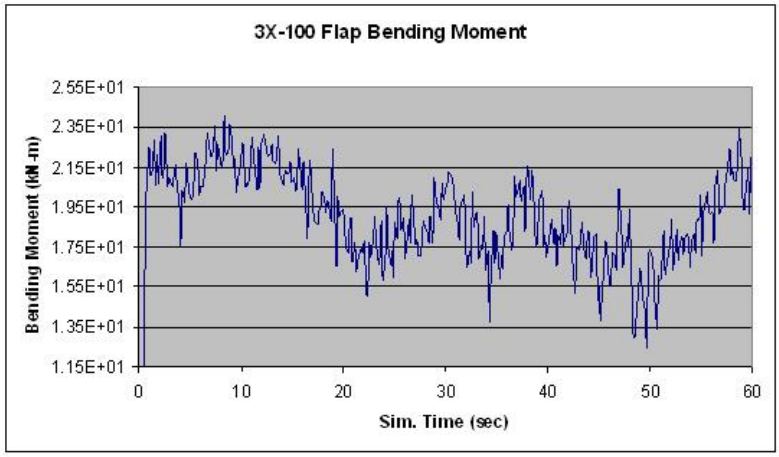

Figure 23: 3X-100 Flap Bending Moment

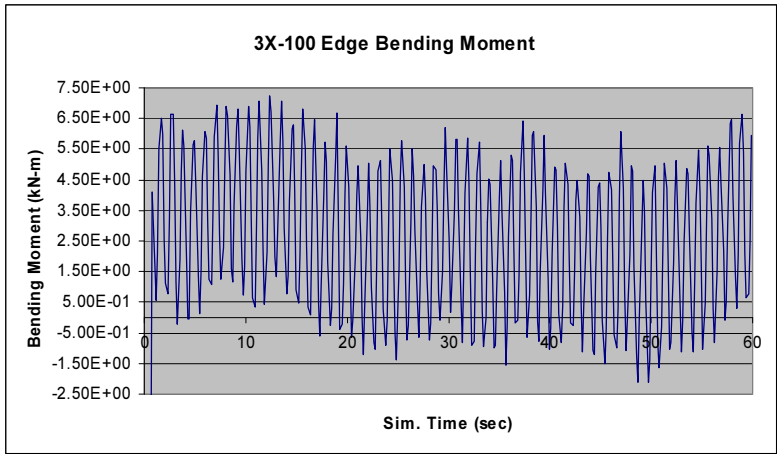

Figure 24: 3X-100 Edge Bending Moment

Stall Region Performance

A secondary analysis was performed for the stall region of the power curve in order to identify the loads for that condition, see Figure 25. The stall region is being defined as the area past the knee of the power curve and occurs at wind speeds higher than 13 m/s. A nominal value of 15 m/s with turbulence intensity "B" was used to determine the loads for this condition. The blade response for the stall region operation can be seen in Figure 27 and Figure 28.

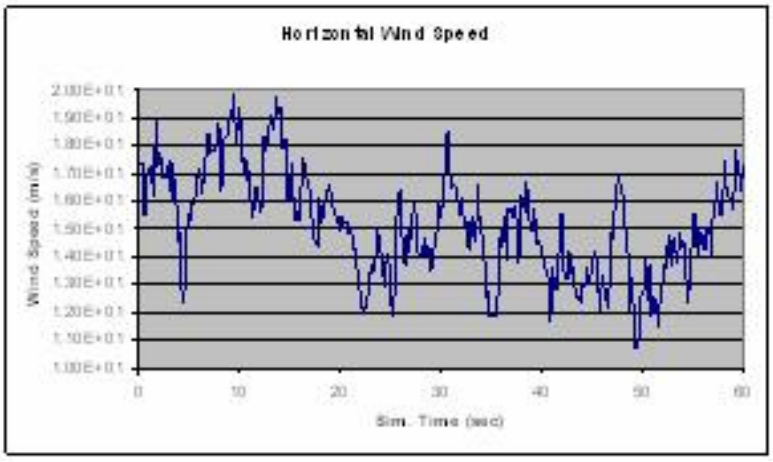

Figure 25: Simulated Wind Speed Data for a 15 m/s, Turb. B.

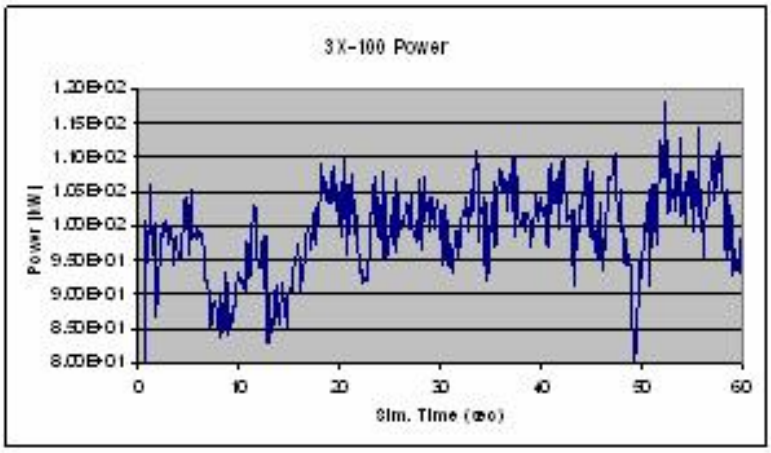

Figure 26: Rotor Power, 15 m/s, Turb. B

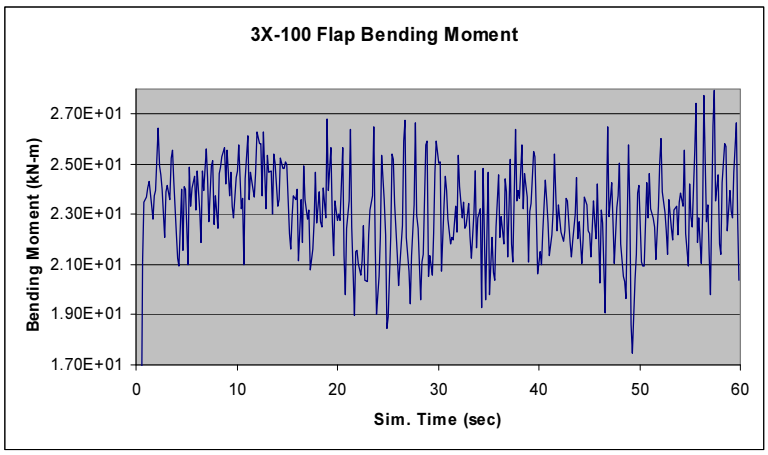

Figure 27: 3X-100 Flap Bending Moment

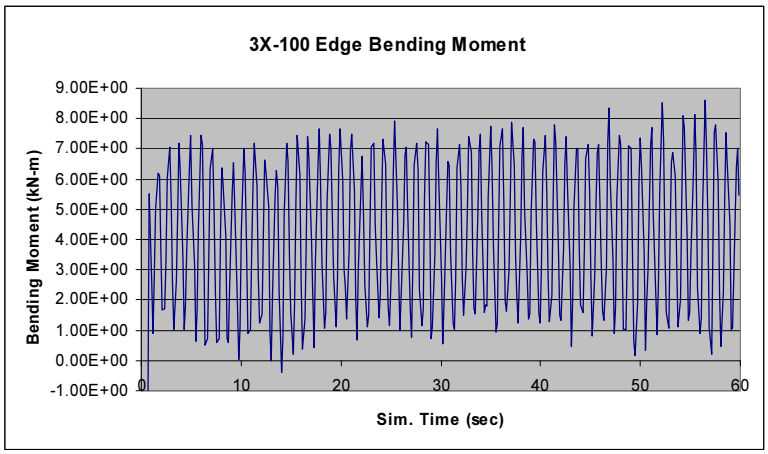

Figure 28: 3X-100 Edge Bending Moment

FIELD DATA ANALYSIS

Background

The field testing campaign began in July 2006 with the erection of the newly modified test bed equipped with the 3X-100 blades, with a second campaign starting in February of 2007. In the initial weeks of the test, all of the instrumentation was calibrated and preliminary checkouts of the new controller algorithms were performed. Once these were completed, the data collection began. Since many components on the machine had been replaced or modified, the machine was only operated during manned hours. This decision did not affect the quality of the test or the outcomes of the data analysis, since the purpose of the test is to understand the performance of the 3TEX material. At this point there were still a few things that were being debugged on the testbed and these limited the amount of data collected. Two yaw drive failures had been experienced and these were determined to be due to pitch angle differences that oscillated the nacelle. After the necessary repairs were made and the blade pitch angles were realigned, data collection resumed during manned hours and in a more conservative wind speed envelope. This was the second part of the campaign.

The initial campaign collected a total of 370 data records that have been analyzed and divided into wind speed bins. The data has been filtered for files that do not have a power production value greater than zero for the entire record in order to not affect the analysis. In addition, if other discrepancies were noticed in the data, those files were disregarded and set aside for further analysis. After filtering all of the data, a total of 120 10-minute records remained for detailed analysis from the first campaign. For the second campaign, 208 files were collected and analyzed and once the same power production filter was used on these files, 167 files remained.

Figure 29: Micon Turbine with 3X-100 Blades

Yaw Drive Problem and Blade Pitch

As mentioned above, we have experienced two yaw drive mechanism failures since the beginning of the test. The PSD plot shown in Figure 30, shows the difference in flap excitation at low and high wind speed. It can be noticed that at the higher wind speed the flap bending PSD depicts a more expected PSD image. After further testing, a possible cause of this problem was determined to be a variance in the pitch angle of the blades.

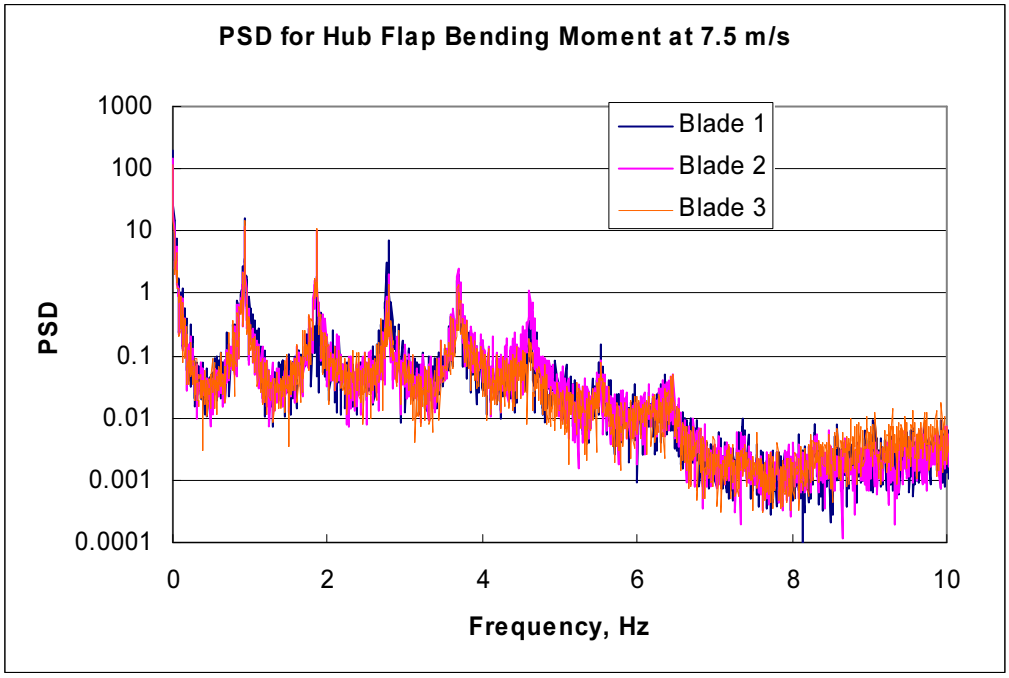

Figure 30: PSD for Hub Flap

Problem:

During field testing of the 3X-100 (3TEX) blades, a strong nacelle oscillation was observed when the machine was in operation. The oscillation was so severe that it may have contributed to the failure of the yaw drive shaft and yaw brake bracket. The vibration was especially noticeable during yawing as the nacelle is yawed without a damper and there is some slop in the yaw drive transmission. Interestingly, this oscillation was more prominent at lower wind speeds than at higher ones. This would tend to rule out a weight imbalance between the blades, as that would cause an oscillation that would only be dependant on rotational speed. Since the Micon is a constant-speed machine, the oscillation would be the same regardless of wind speed. This suggested that the problem was aerodynamic in nature.

Figure 31 presents the measured hub flap bending moments for all three hubs as a function of wind speed. A considerable difference in the measurements can be seen. In particular, the slopes are different, with a maximum difference occurring at 6-7 m/s and decreasing with higher wind speeds.

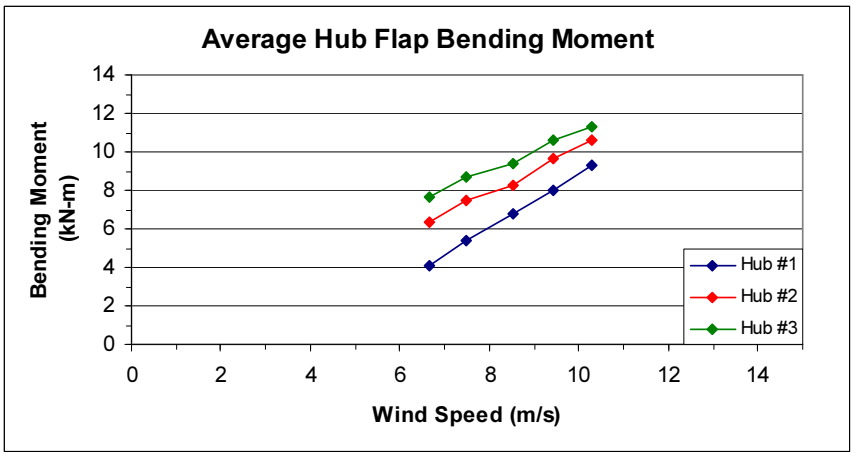

Figure 31: Hub flap bending moments.

Figure 32 shows a similar plot but with edge moments shown. The differences here are not as large. This is not unexpected, given that most of the lift and drag effects on turbine blades are translated into thrust loads on the rotor with a smaller portion going towards rotor torque. However, similar trends are evident in this plot: differences in the three blades growing smaller with increasing wind speed.

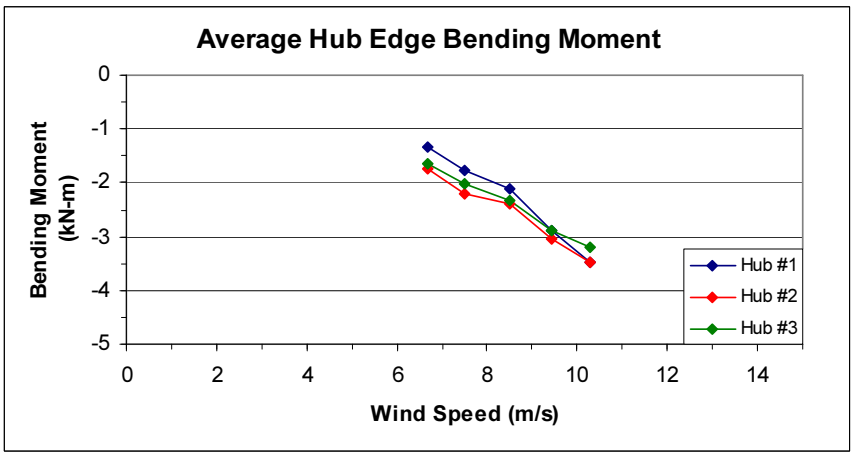

Figure 32: Hub edge bending moments.

Since the flap loads were shown to be of greater concern, it is useful to examine how the differences in flap loads shown in Figure 31 would be translated to moments on the turbine. Figure 33 shows a calculation of the yaw and fore-aft moments that would be present given the imbalance in flap loads that was measured. The moments are plotted against rotor position with 0º corresponding to hub 1 being vertically upright. Side-to-side moments would obviously not be affected by a flap load imbalance and thus are not shown. Naturally, the phases of the two responses are separated by 90º. The maximum moment is seen to be nearly 4 kN-m, a large amount considering that the yaw drive is designed around a 2 kN-m design load.

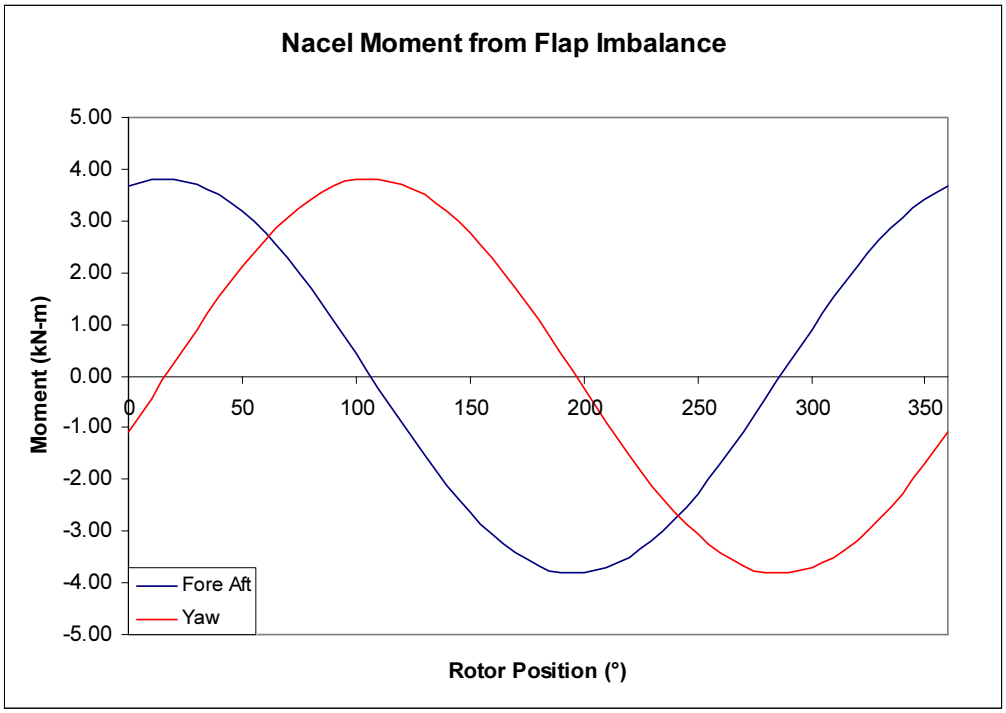

Figure 33: Calculated oscillatory moment on nacelle.

In light of this and other evidence, a determination was made that the oscillation was being caused by an aerodynamic difference between the three blades. The possible cause of this aerodynamic difference was reasoned to be either a discrepancy in the pitch settings of the blades or an actual difference in the geometries of the blades.

Solution:

To alleviate this problem, the pitch angle was measured at four spanwise locations on each blade. These measurements would show whether the pitch was off globally or locally along the blade and answer the question of why there existed an aerodynamic difference between the blades.

The pitch angles were measured with a digital inclinometer located on a two foot level. The rotor was rotated so that the blade to be measured was pointing out horizontally. The level was placed on the high pressure surface of the blade, contacting at the trailing edge and along the blade surface near mid chord. The measurements were corrected for the tilt of the nacelle and the difference between the measured angle and the true pitch angle at that blade station. The results are plotted in Figure 34, along with the desired pitch distribution based on the design calculations. The results show that all of the blades had the same geometric characteristics, but the blades on hub 2 and hub 3 were rotated significantly from the desired pitch setting. Hub 1 was found to be quite close to the desired orientation.

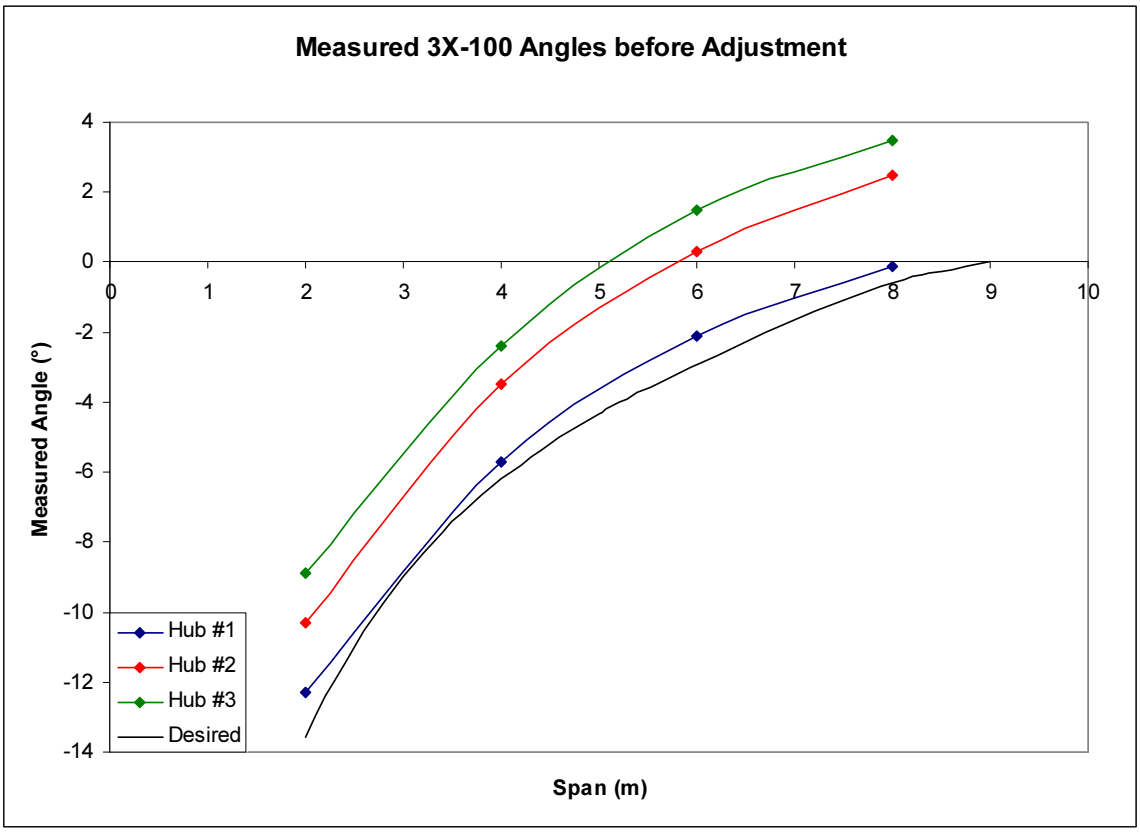

Figure 34: Measured 3X-100 initial pitch angles.

Having the pitch angle set higher than desired yields a blade that stalls earlier and thus should result in poor performance. Figure 35 shows the power generated by the 3X-100 blades in their sub-optimal state as compared to the power that was predicted through a FAST analysis. This hypothesis is affirmed by the data collected, as the turbine with the blades in the initial configuration was seen to be producing significantly less power than expected.

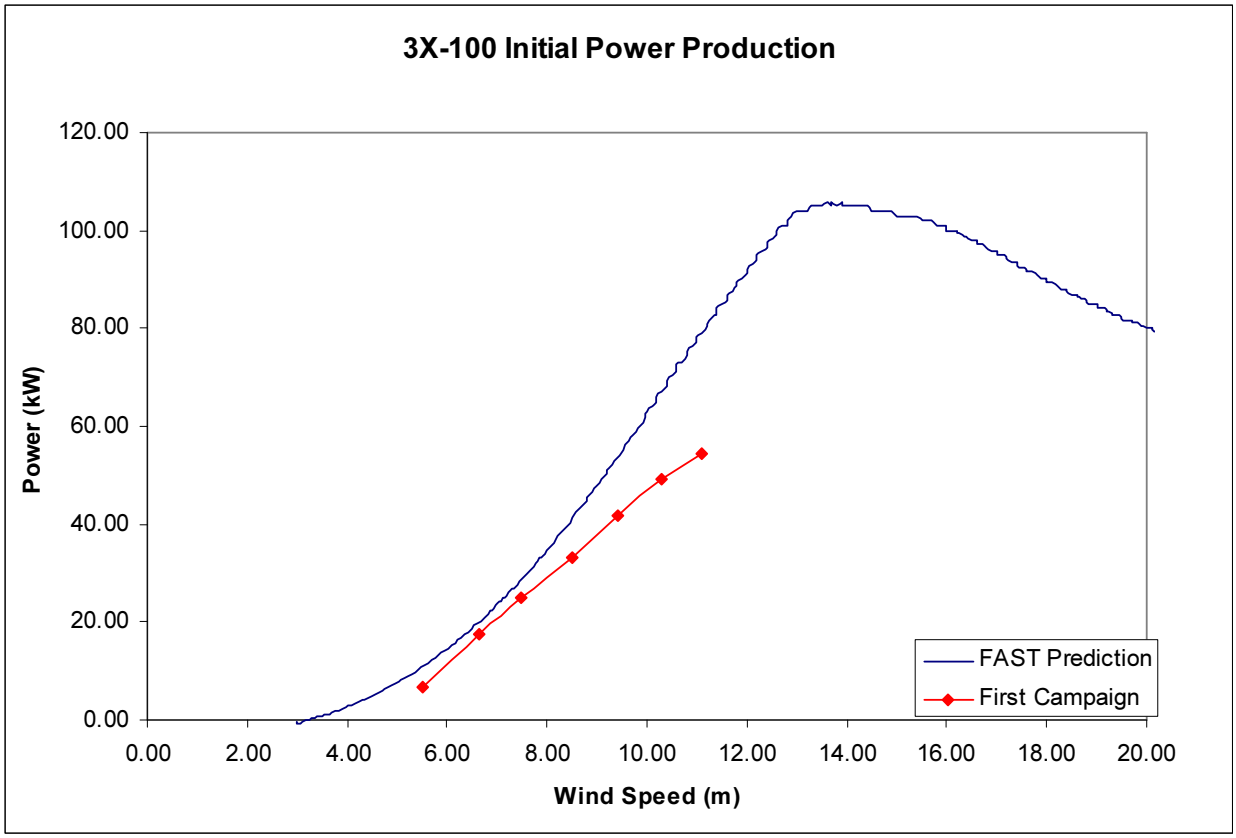

Figure 35: 3X-100 initial power production.

In light of these results, it was decided that the pitch angle would be changed on the blades attached to hubs 2 and 3.

Results:

The pitch angles of the altered blades were measured again after the adjustments were made and the results are shown in Figure 36. The blades on hub 2 and 3 are seen to be much more closely aligned with the desired pitch angle. However, the plot shows a difference remaining between the adjusted blades and the blade that was left unchanged. The blade on hub 1 was not measured after the other blades were changed. Furthermore, the blades were originally measured in the afternoon on a warm day, while the second set of measurements were taken in the morning on a cooler day. Given the small measured differences in pitch we concluded that it was futile to attempt to get any better adjustment

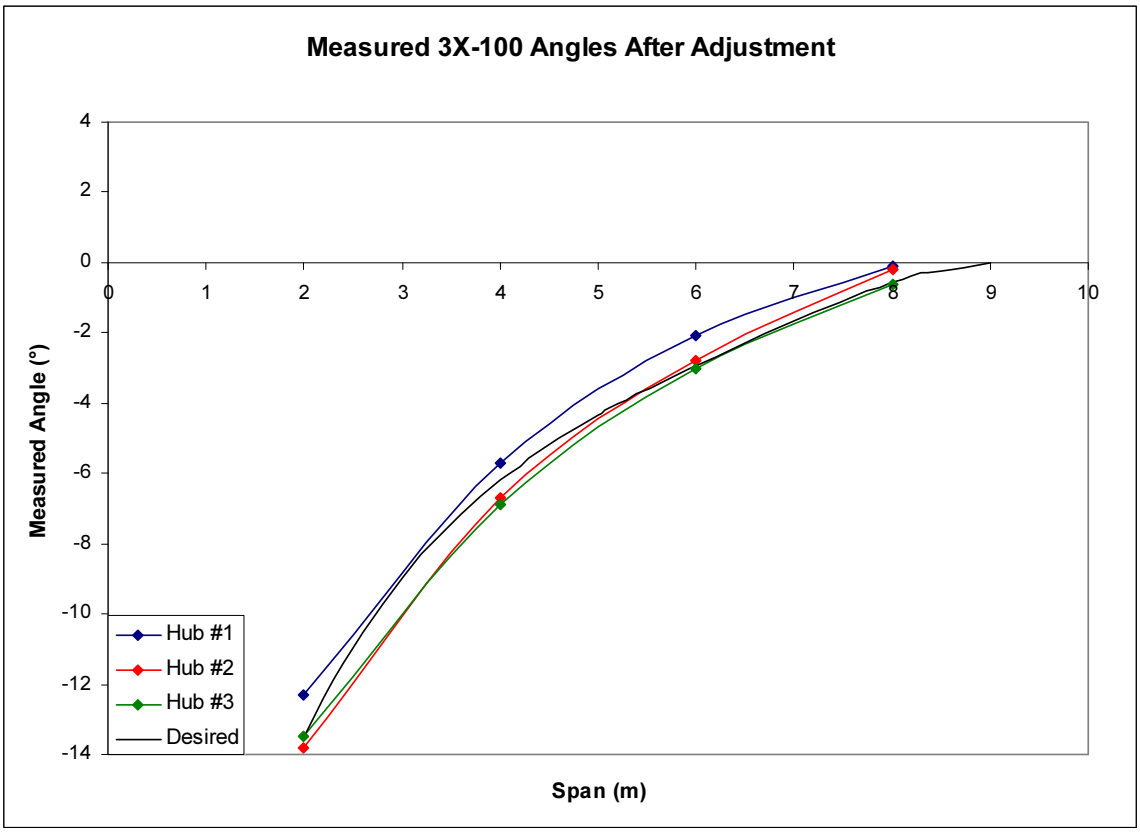

Figure 36: 3X-100 pitch angles after adjustment.

After adjustment of the blades, the oscillation ceased.

Data Summary

All of the data records have been analyzed and divided into wind speed bins. As mentioned earlier, the data has been filtered for files that do not have a power production value greater than zero for the entire record in order to not affect the analysis. After filtering, the initial campaign had a total of 120 10-minute records that remained for detailed analysis. The second campaign had a total of 167 files. A graph of the total number of records collected in each bin is shown in Figure 37.

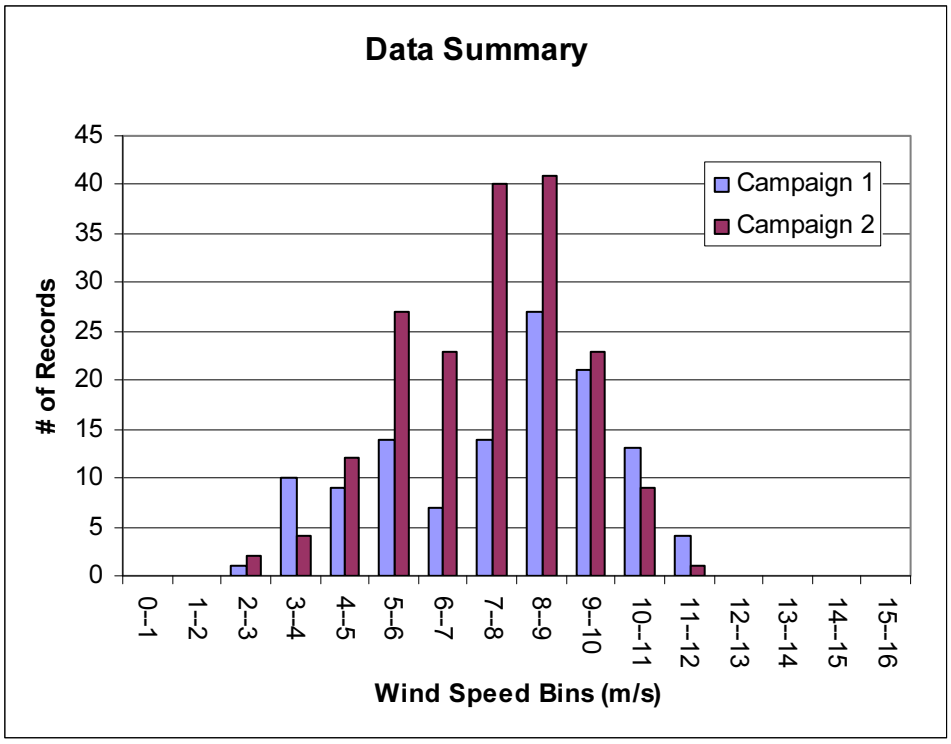

Figure 37: Wind Speed Bin Comparison

Data Analysis

Time Series Data Campaign 1 and Campaign 2

"Strip charts" of typical time series data for the two campaigns are shown below in Figure 38 thru Figure 49. The two campaigns have similar mean wind speeds (9.76 m/s) with a turbulence intensity of 13.58% for the first campaign and 15.27% in the second campaign. These particular strip charts were chosen because the wind speed remained relatively constant for the 10-minute record.

The hub height wind speed, electrical power, wind direction, blade flap and edge bending, and tower bending are shown below for both campaigns. The inflow and response of the turbine are characterized by these data.

First Campaign

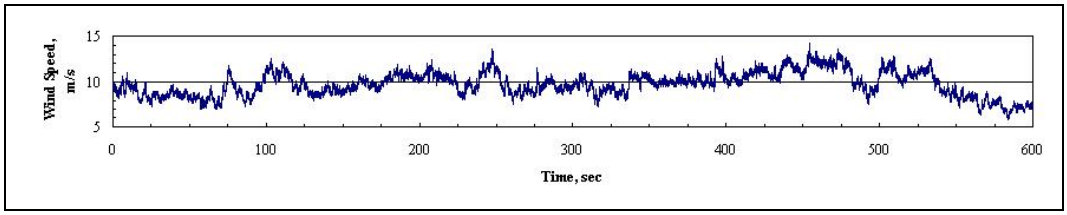

Figure 38: Hub Height Wind Speed

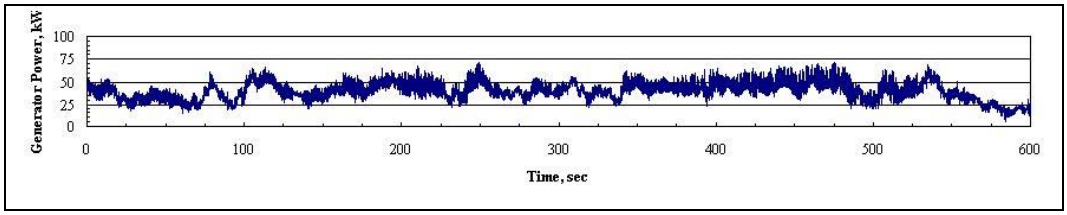

Figure 39: Electrical Power

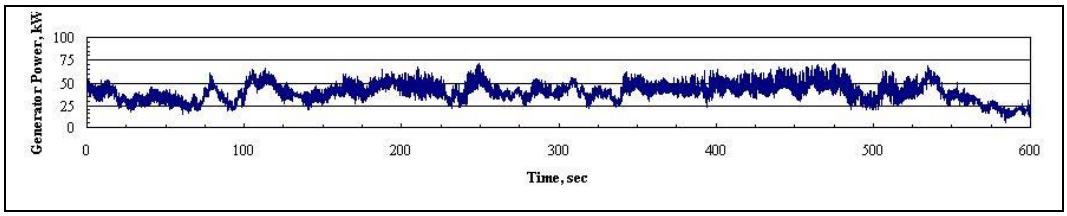

Figure 40: Wind Direction

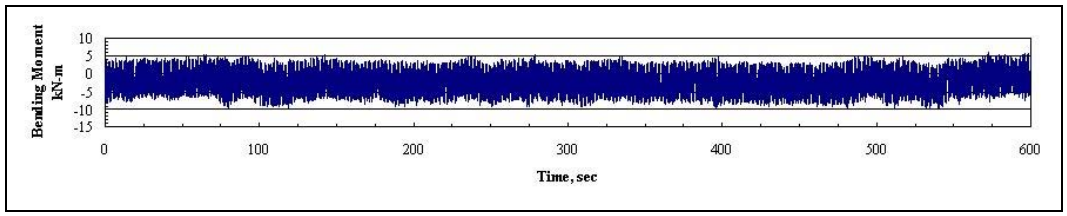

Figure 41: Root Flap Bending

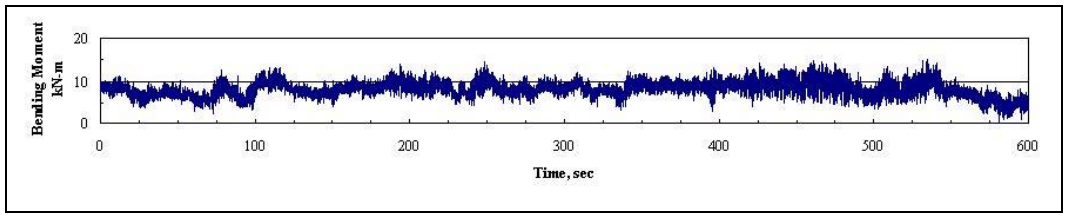

Figure 42: Root Edge Bending

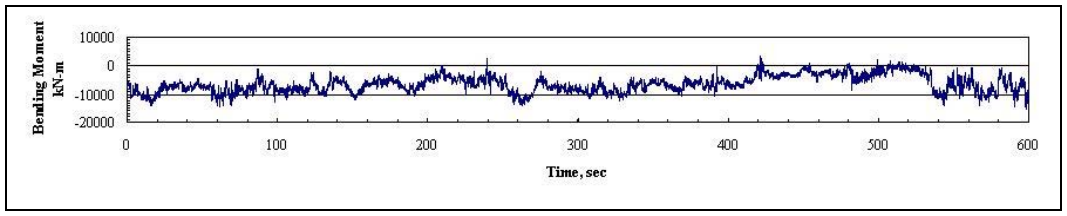

Figure 43: Down Wind Tower Bending

Second Campaign

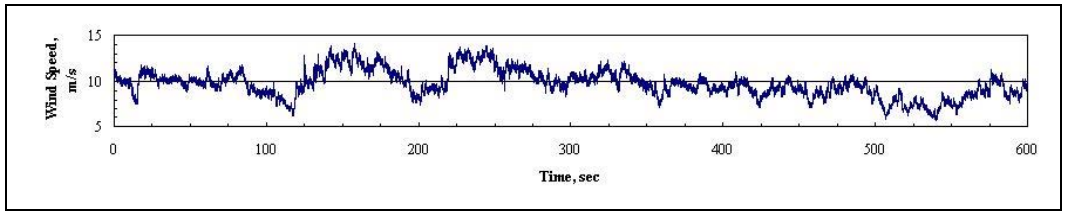

Figure 44: Hub Height Wind Speed

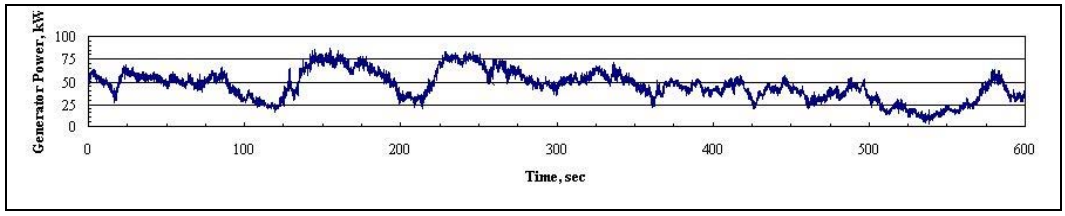

Figure 45: Electrical Power

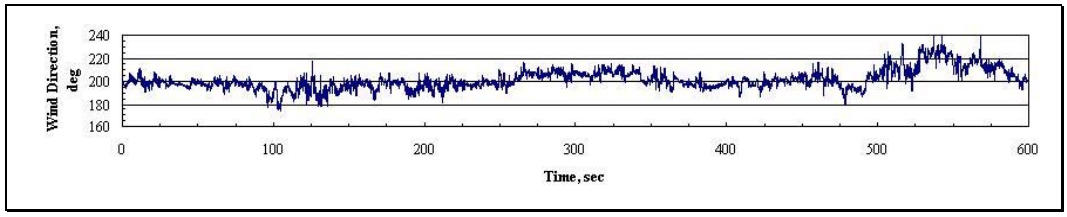

Figure 46: Wind Direction

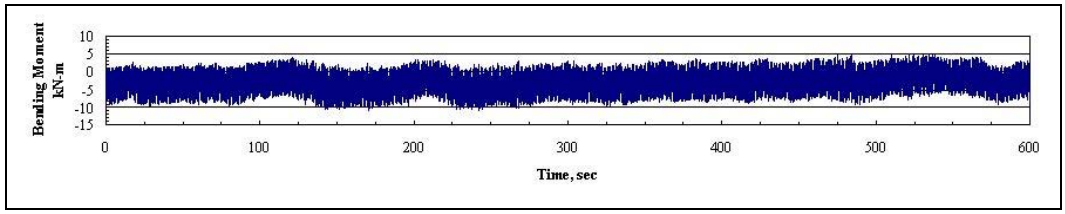

Figure 47: Root Flap Bending

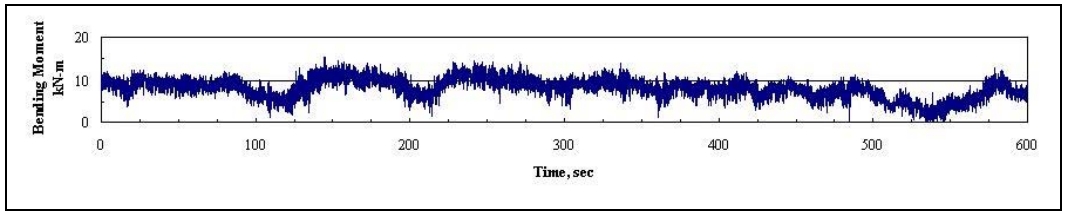

Figure 48: Root Edge Bending

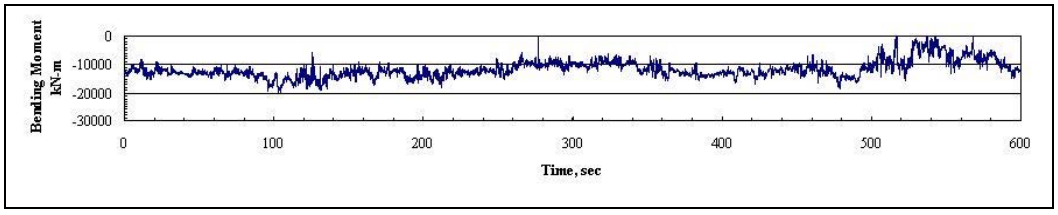

Figure 49: Tower Bending

Power Production

Power production for the two campaigns is shown in Figure 50 and Figure 51. These 10 minute average power curves are a function of wind speed. Averaged generator power as well as instantaneous minimum and maximum data are plotted. A comparison between the two curves can be seen in Figure 52.

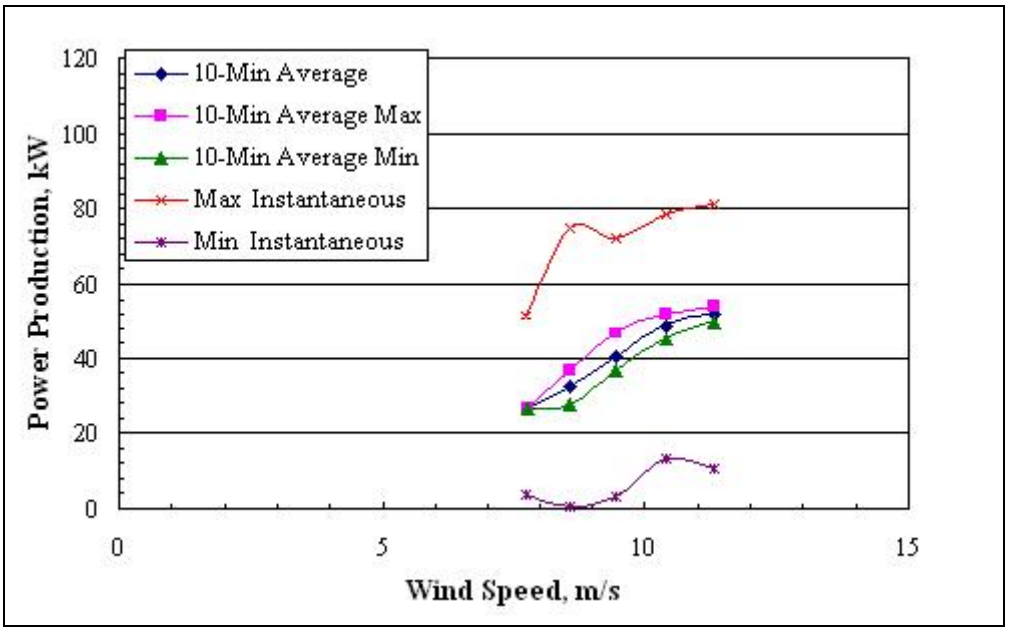

Figure 50: Power Production First Campaign

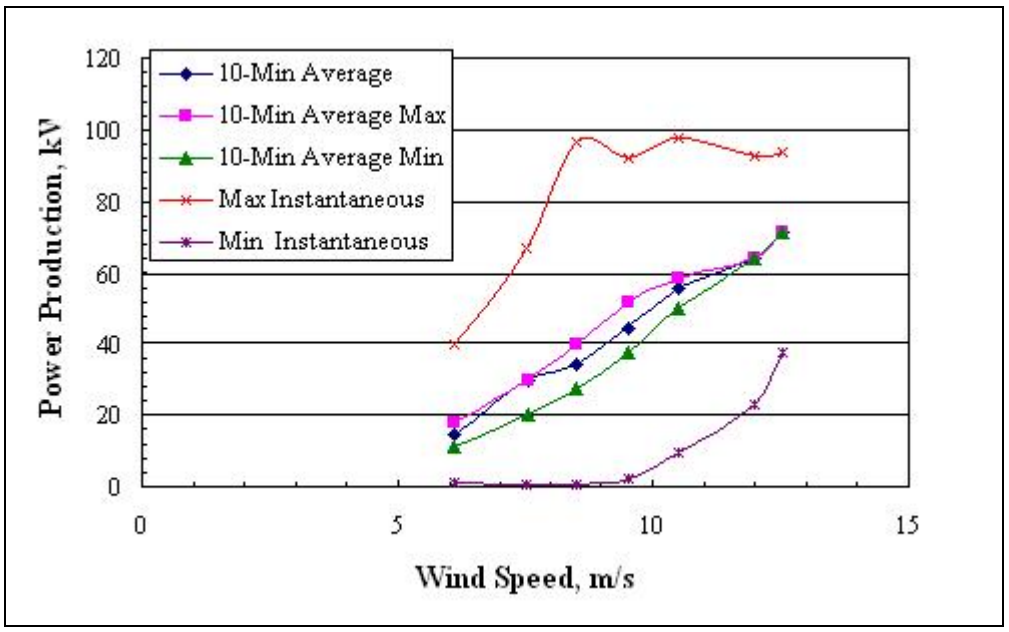

Figure 51: Power Production Second Campaign

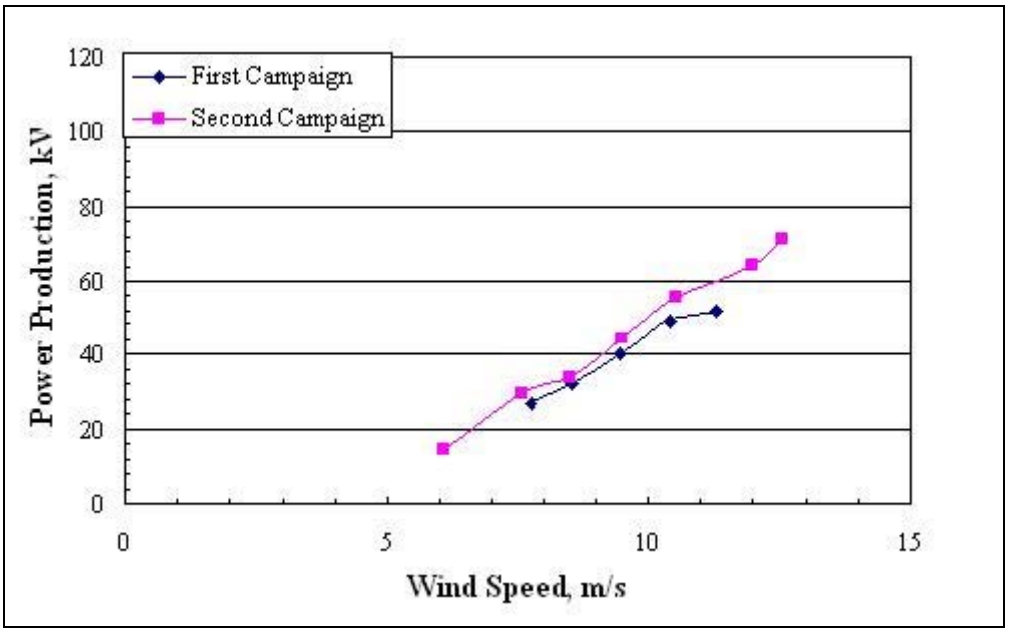

Figure 52: 10-miinute Average Power Production Comparison

Load Spectrum

The mechanical response of the turbine to the various inflow conditions can be described in a number of different ways for campaigns 1 and 2 respectively. The hub edge bending loads measured at the root of each blade are shown as a function of wind in the following plots, Figure 53 and Figure 54.

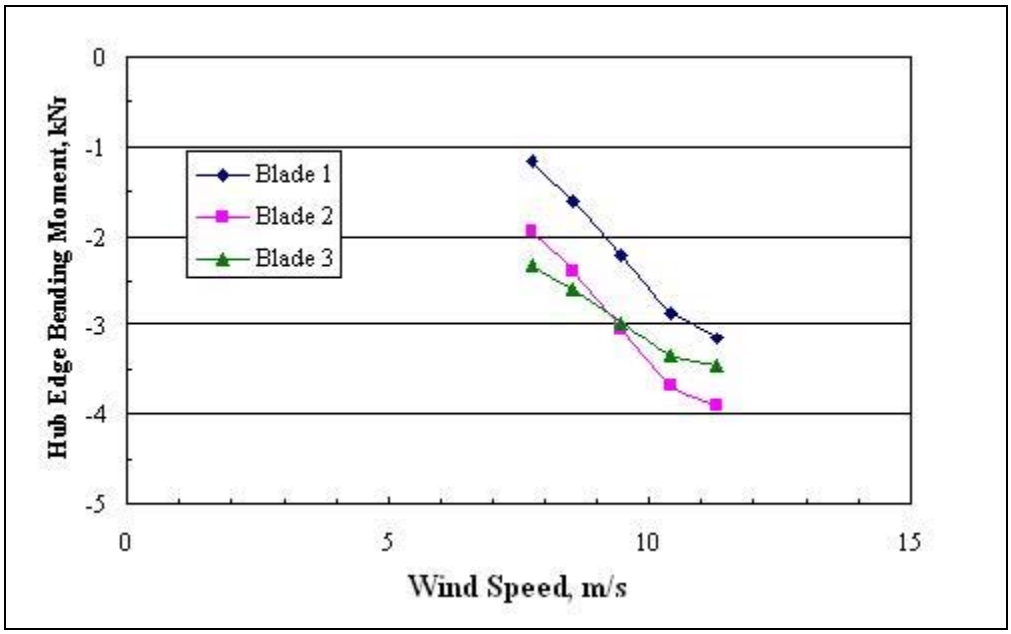

Figure 53: 10-minute Average First Campaign Hub Edge Bending Moments

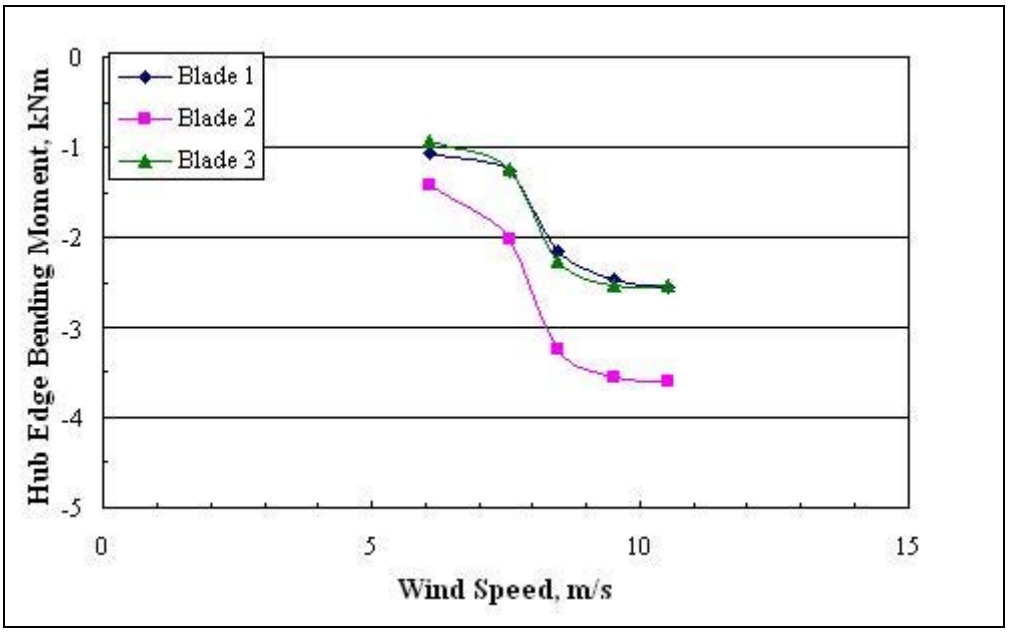

Figure 54: 10-minute Average Second Campaign Hub Edge Bending Moments

The flapwise bending loads measure at the root of each blade are shown as a function of wind speed between campaign 1 and campaign 2 can be seen in the following plots. In Figure 55 and Figure 56, the hub flap bending moments observed for all 10-minute data records have been analyzed.

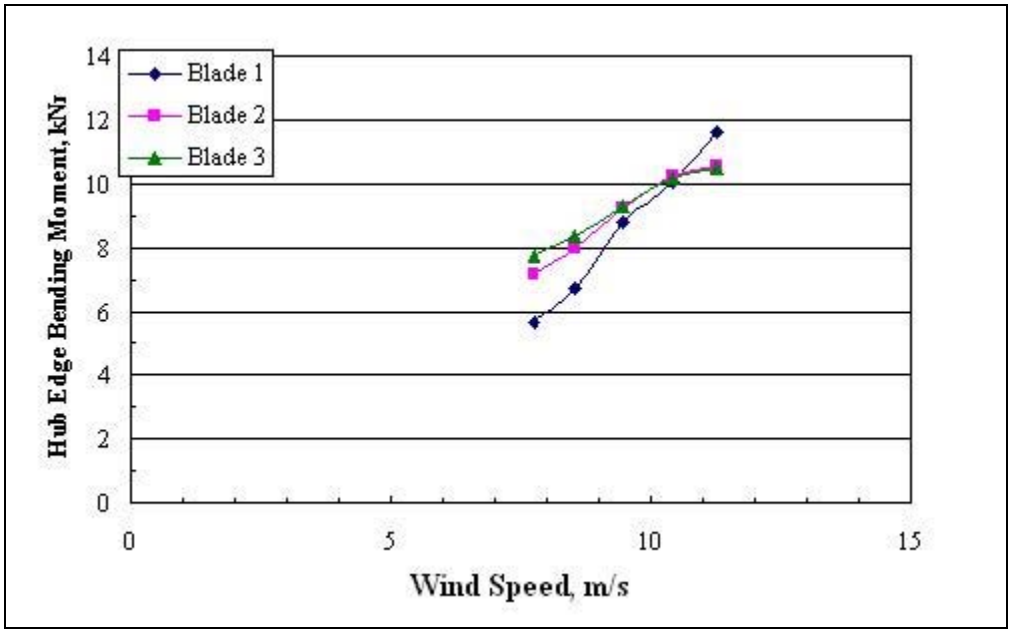

Figure 55: 10-minute Average First Campaign Hub Flap Bending Moment

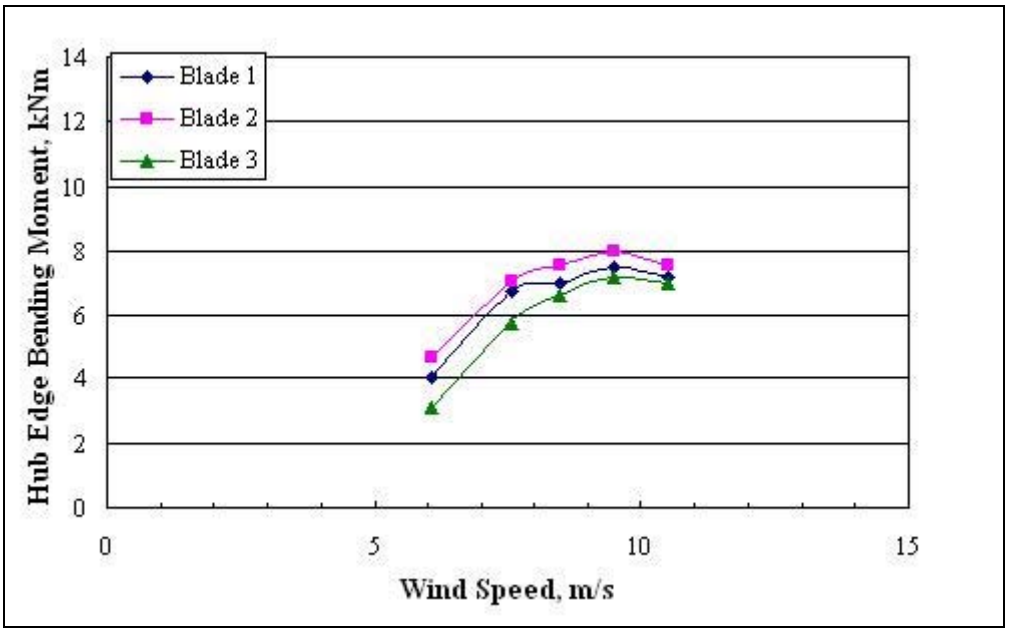

Figure 56: 10-minute Average Second Campaign Hub Flap Bending Moment

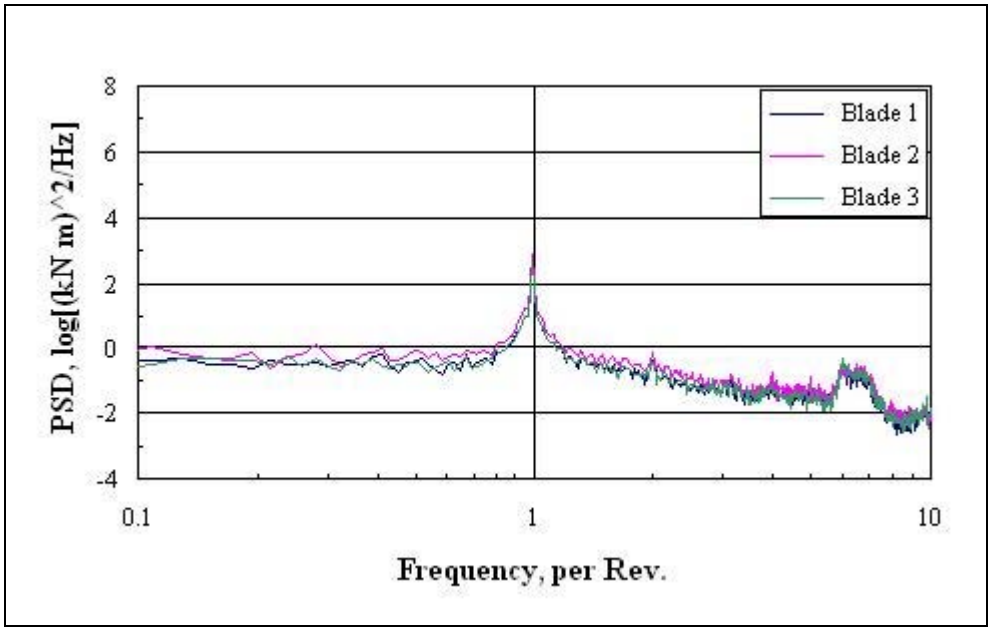

Figure 57: First Campaign PSD for 7 m/s Wind Speed

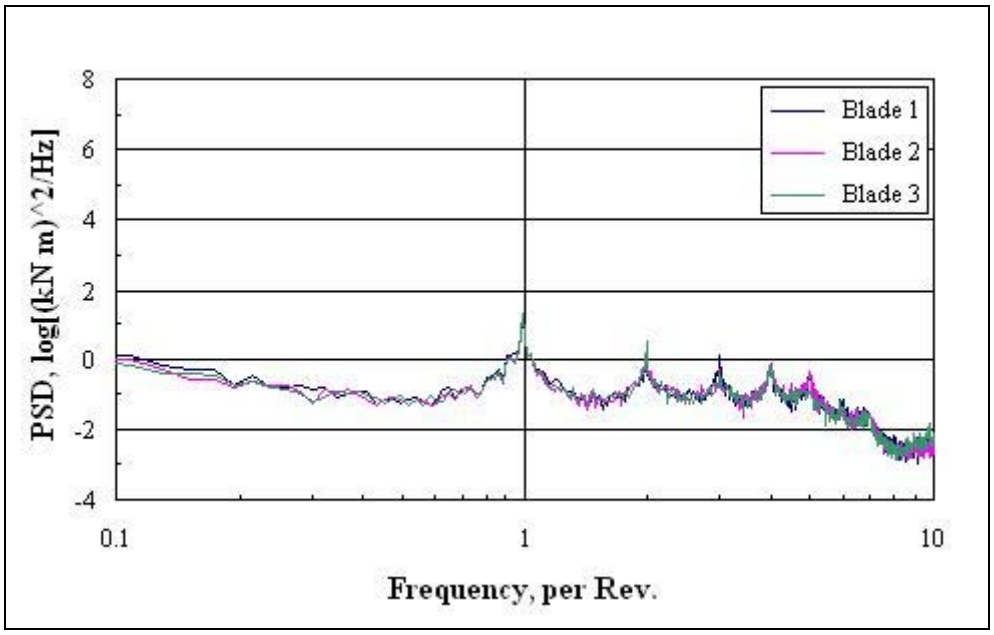

Figure 58: First Campaign PSD for 7 m/s Wind Speed

To determine the frequency content of the time-series data shown in the following figures, the Power Spectral Density (PSD's) for the blade loads were determined. A comparison of the blade PSD plots is shown in the figures below. The plots have been normalized to the average rotational rate for the 10minute data segment used to conduct this analysis. The NREL developed GPP code was used to perform these calculations. The first two PSD plots, Figure 57 and Figure 58, are from the first campaign with a 7 meter per second average wind speed. The second set of PSD plots is from the second campaign at a 7 meter per second wind speed, see Figure 59 and Figure 60.

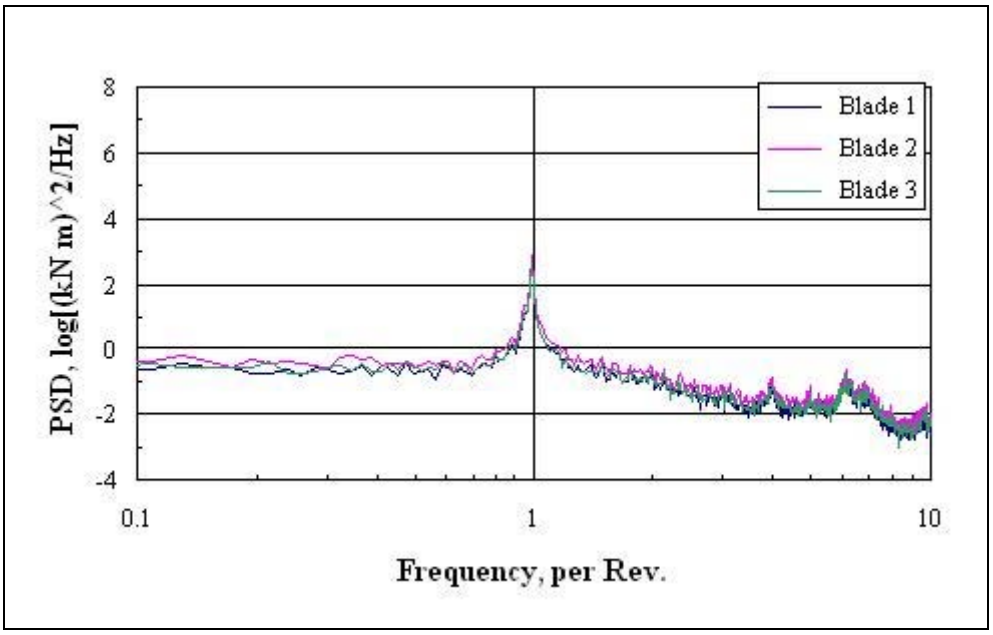

Figure 59: Second Campaign PSD for 7 m/s Wind Speed

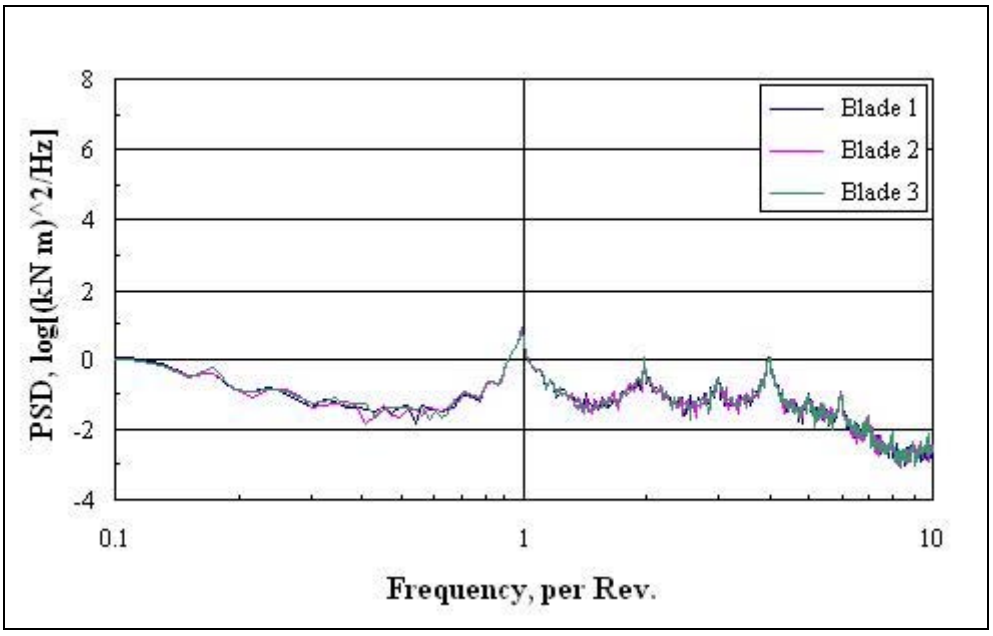

Figure 60: Second Campaign PSD for 7 m/s Wind Speed

The azimuth averages of the flap and edge bending moments for the two campaigns are shown in Figure 61and Figure 62. It can be seen from Figure 63 and Figure 64 that the flap bending moments are less in the second campaign.

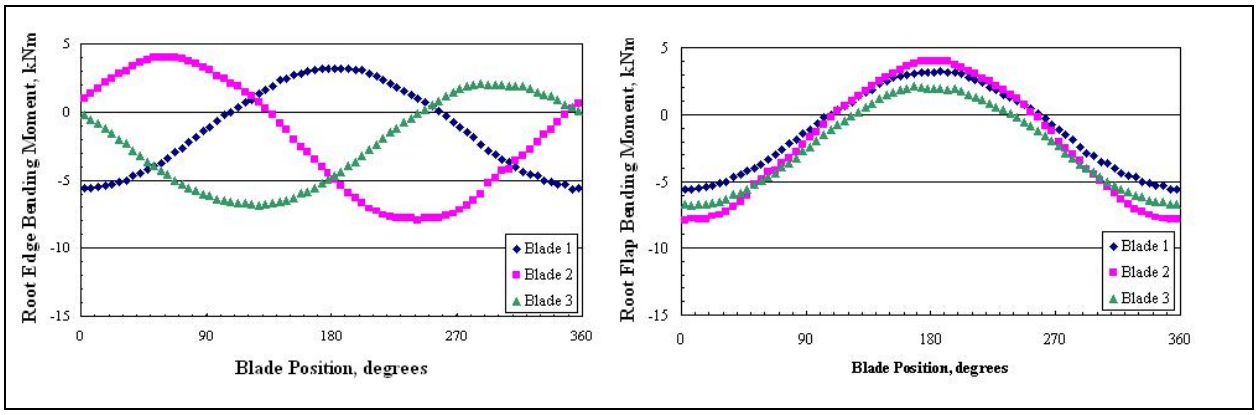

Figure 61: First Campaign Azimuth Average Edge and Flap Bending Loads

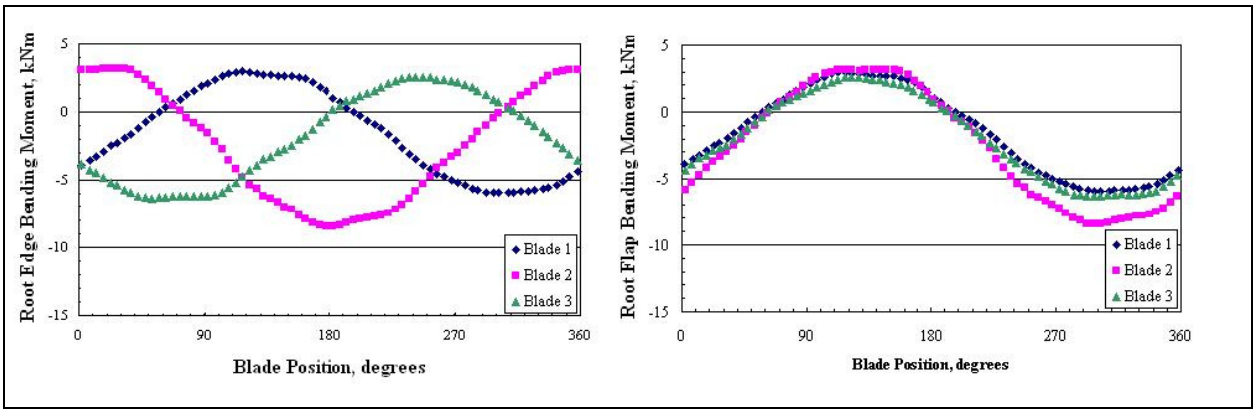

Figure 62: Second Campaign Azimuth Average Edge and Flap Bending Loads

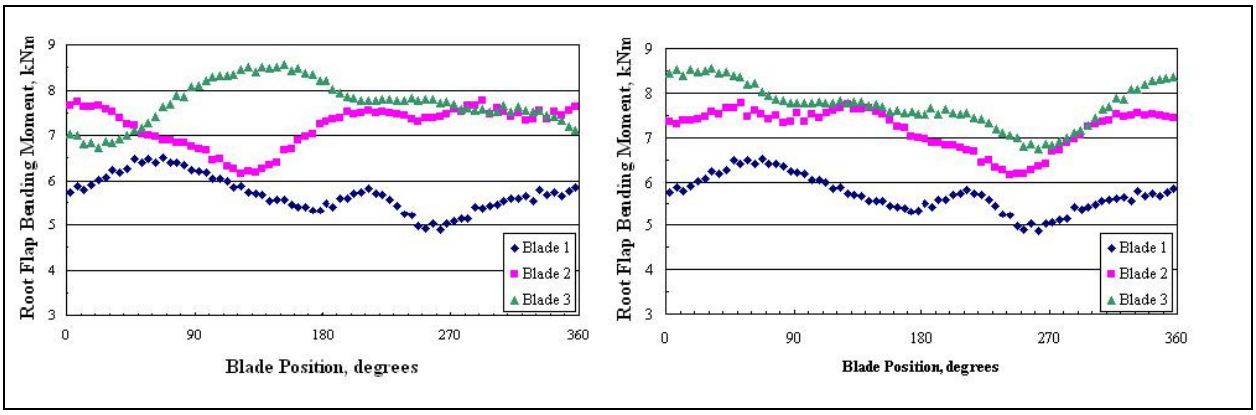

Figure 63: First Campaign Azimuth Average Flap Bending Loads

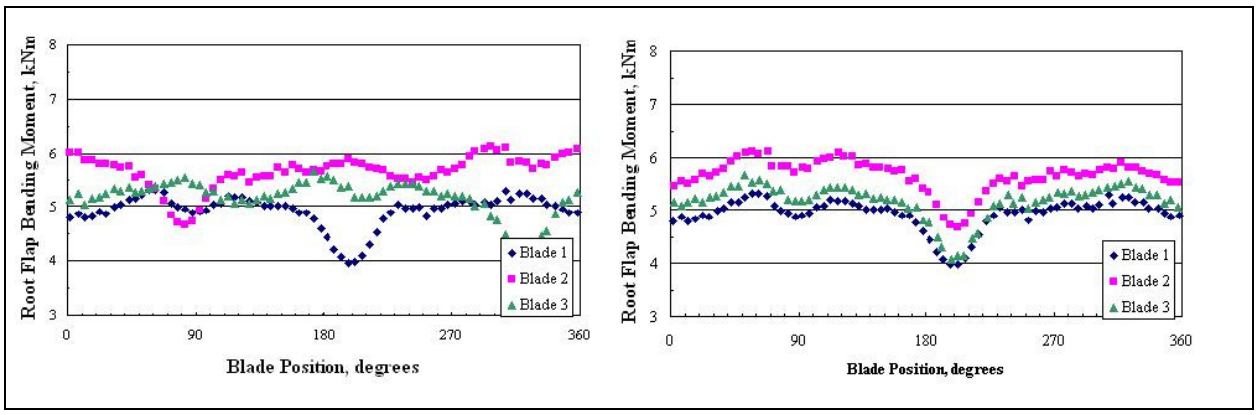

Figure 64: Second Campaign Azimuth Average Flap Bending Loads

Fatigue Spectra

Typical fatigue load spectra are shown below for three wind speed bin regions. These data have been rainflow counted using the CRUNCH computer code. The data has been normalized to 1000 seconds. For this analysis, the data segments were concatenated together and then counted. Cycles still open at the end of the counting procedure were closed and counted as a full cycle.

Data are presented here for the entire 120 10-minute records of the first campaign as well as the 167 records in the second campaign. As discussed in previous work by Sutherland, Zayas and Sterns, these comparisons illustrate the importance of long-term data sets. Previous data has illustrated that the extrapolation of relatively short-term spectra to long-term spectra for blade bending is consistent with measured data. They also showed that the high-stress tail of the fatigue load distribution for the blades continues unabaded for the even the longest records. The current data are consistent with these observations.

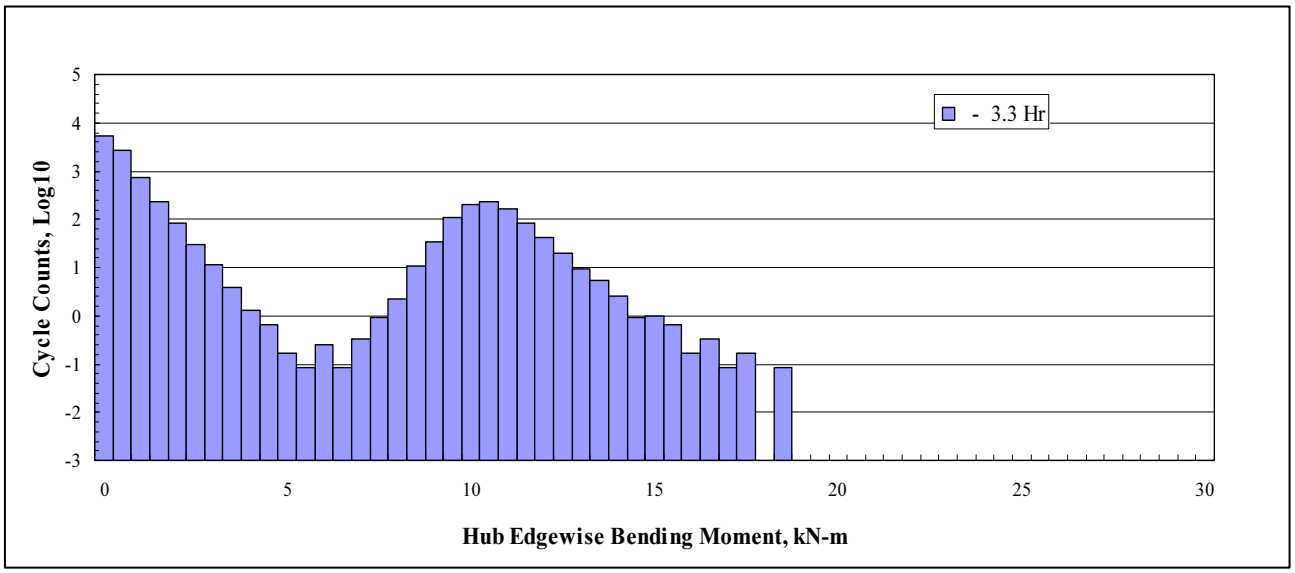

Figure 65: Campaign 1 Edge rainflow count for 7-9 m/s Wind Speeds

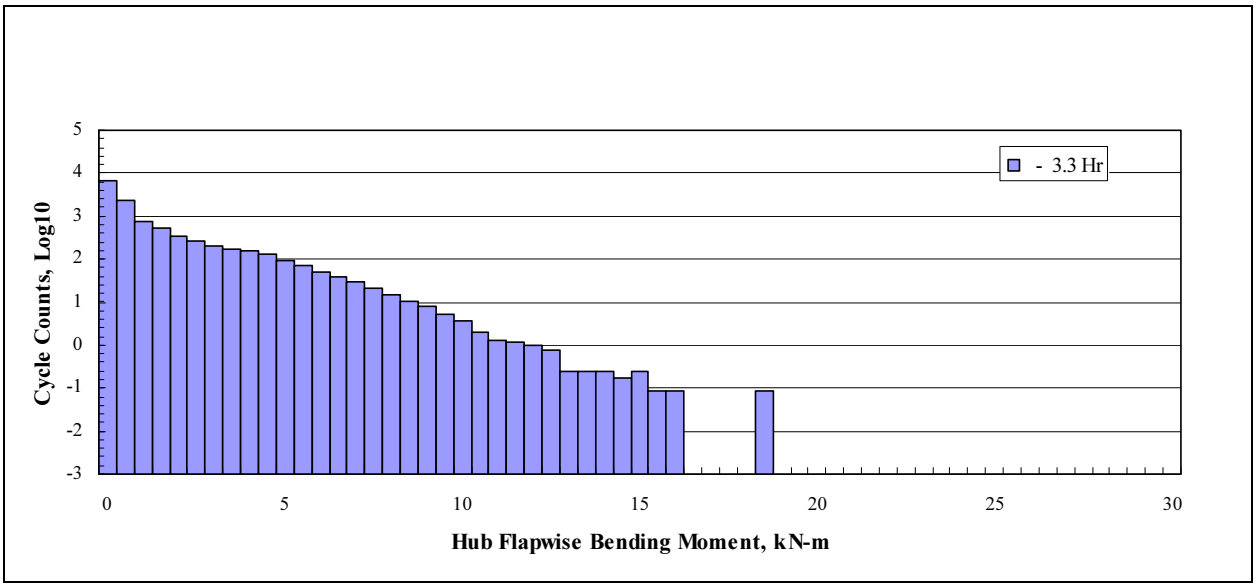

Figure 66: Campaign 1 Flap rainflow count for 7-9 m/s Wind Speeds

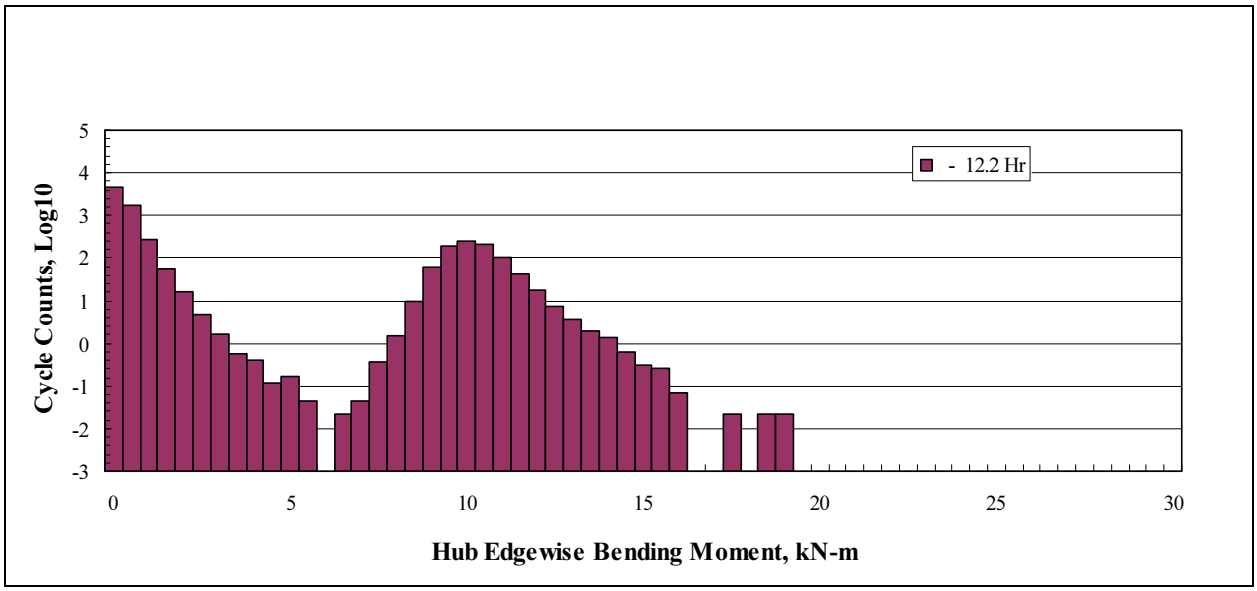

Figure 67: Campaign 2 Edge rainflow count for 7-9 m/s Wind Speeds

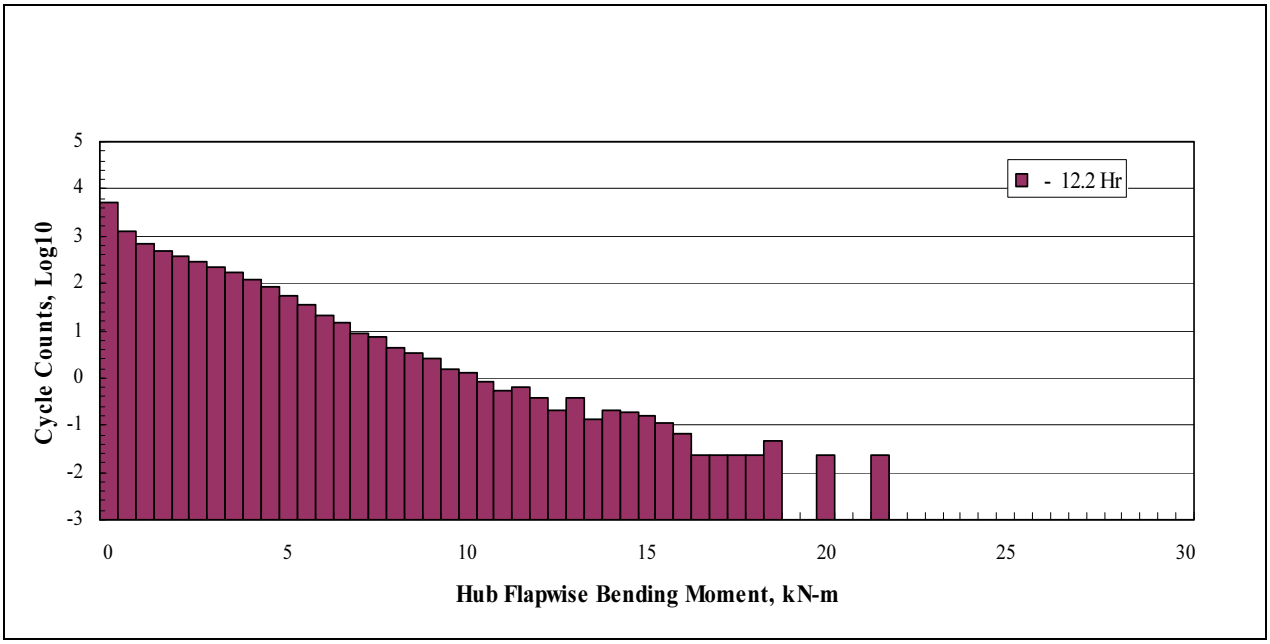

Figure 68: Campaign 2 Flap rainflow count for 7-9 m/s Wind Speeds

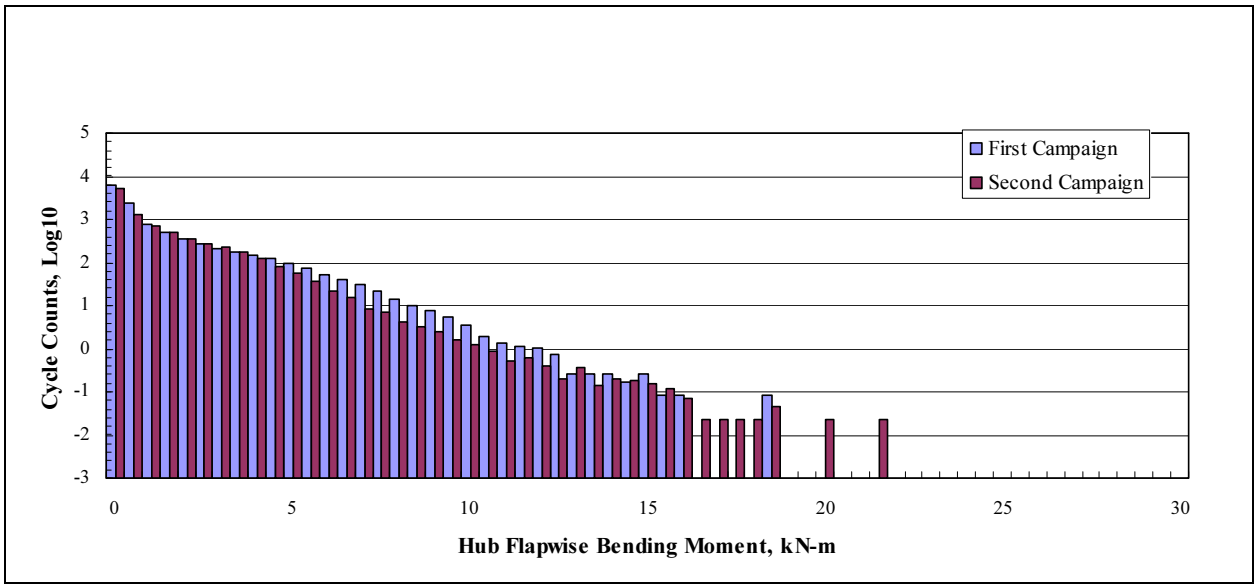

Figure 69: Comparison of Blade 3 Flap Bending Moments

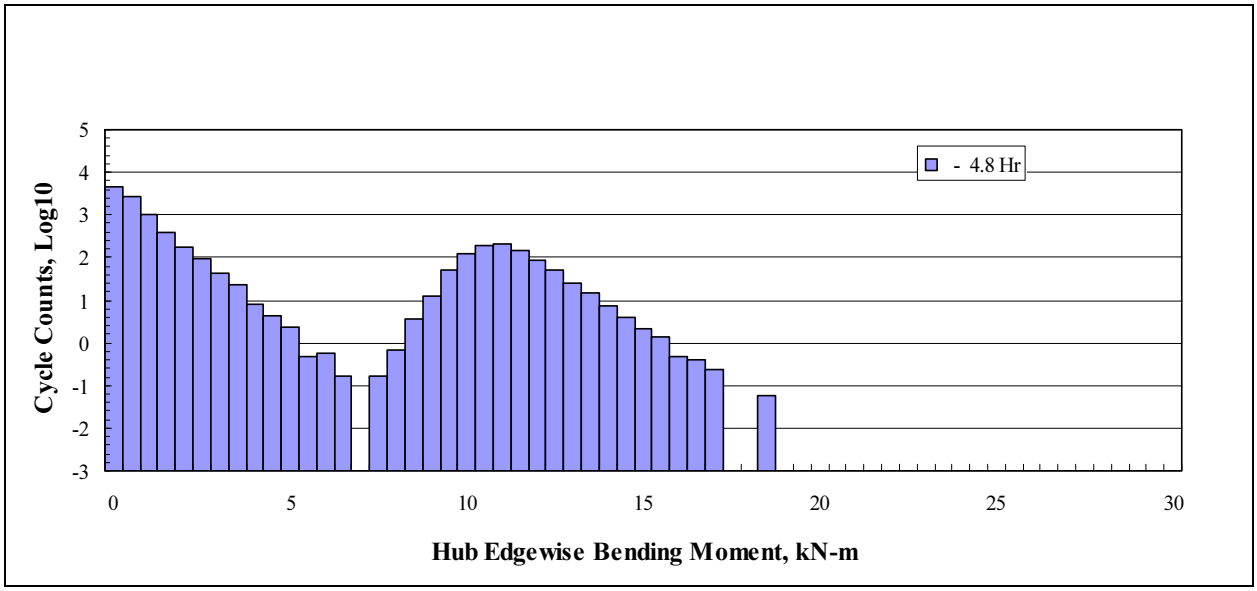

Figure 70: Campaign 1 Edge rainflow count for 9-11 m/s Wind Speeds

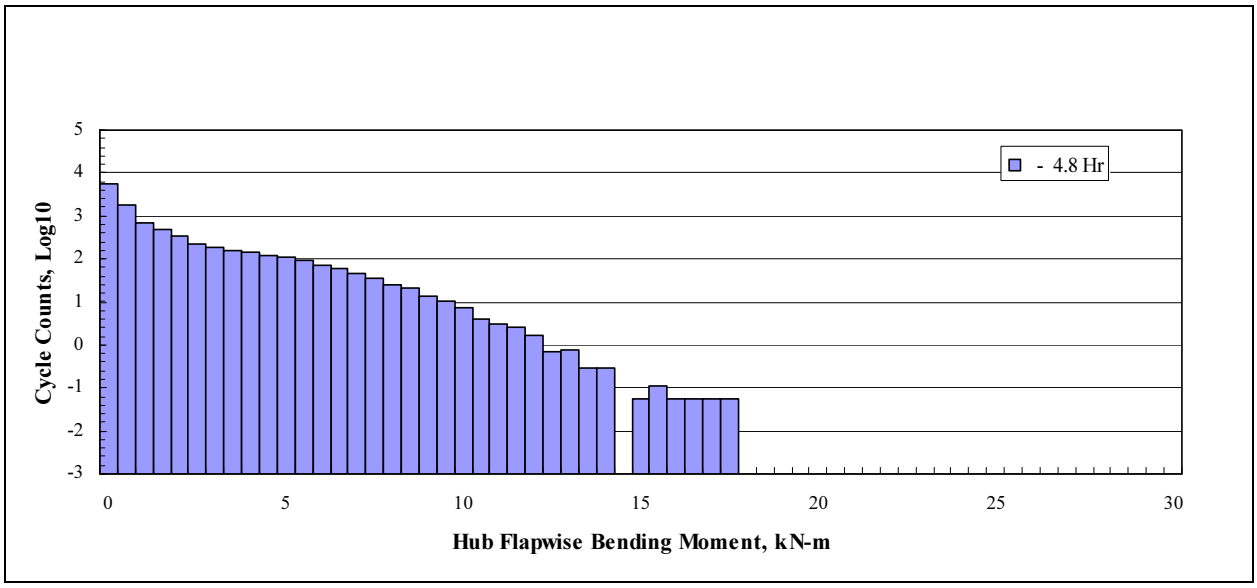

Figure 71: Campaign 1 Flap rainflow count for 9-11 m/s Wind Speeds

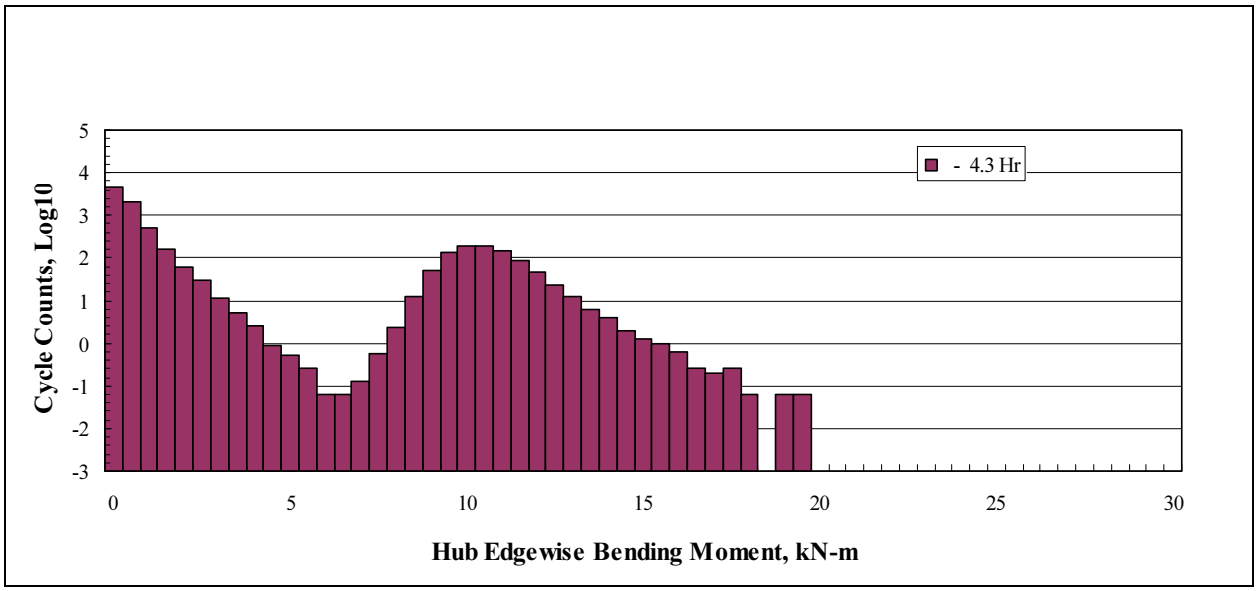

Figure 72: Campaign 2 Edge rainflow count for 9-11 m/s Wind Speeds

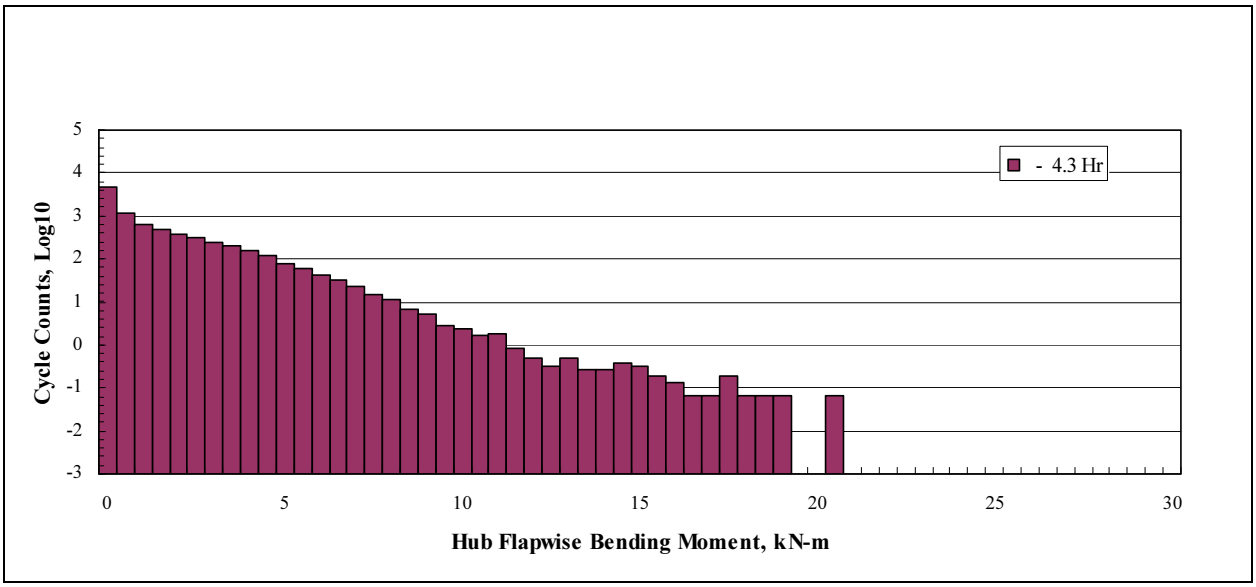

Figure 73: Campaign 2 Flap rainflow count for 9-11 m/s Wind Speeds

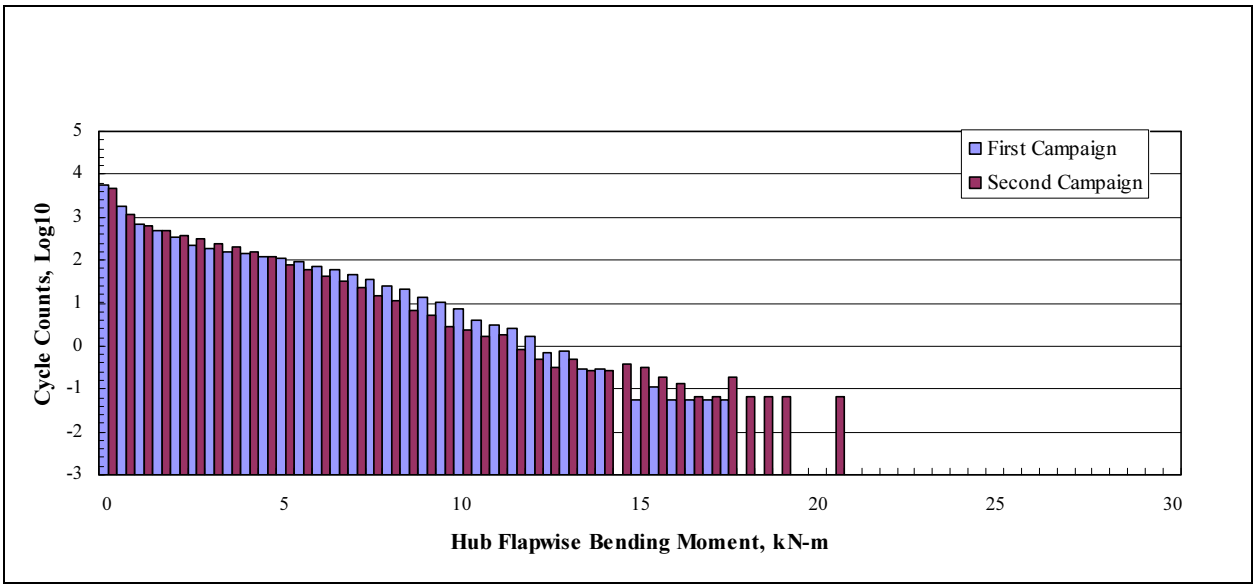

Figure 74: Comparison of Blade 1 Flap Bending Moments

CONCLUDING REMARKS

This report describes the test of the 3 TEX blades, the instrumentation and infrastructure that has been developed to monitor the Micon turbines and their inflow at the Bushland test site. The two campaigns were kept separate due to the different pitch angles of the blades that affected power production and blade loads. Power production in the second campaign was improved over the first campaign as the blades did not reach stall at low wind speeds. From the PSD plots, the material being tested has good damping, better than equivalent fiberglass, and it did not excite any of the fundamental frequencies. Comparison between the loads experienced by the CX-100 cannot be done at this time, as that testing has not been finished.

REFERENCES

1. Zayas, J.R., Jones, P.L., and Ortiz-Moyet, J., "Accurate GPS Time-Linked Data Acquisition System (ATLAS II) User's Manual," SAND2004-0491 February 2004.

2. Met One, Met One Instruments Inc., 1600 Washington Blvd., Grants Pass, OR 97526. http://www.metone.com/index.htm

3. Applied Technologies, Applied Technologies Inc., 1120 Delaware Ave. Longmont, CO 80501. http://www.apptech.com/index1.html

4. Yellow Springs Instruments, Inc., 1700/1725 Brannum Lane Yellow Spring, OH 45387. http://www.ysi.com/index.html

5. Micro Measurements, Vishay Measurements Group Inc., Micro Measurements Division, Raleigh, NC 27611. http://www.vishay.com/company/brands/micromeasurements/

6. Crossbow Technology, Incorporated. 4145 N. First Street, San Jose, CA 95134. http://www.xbow.com

7. Computer Conversions, Computer Conversions Corporation, 6 Dunton Court East Northport, NY 11731 USA. http://computerconversions.com/index.html

8. Ohio Semitronics, Ohio Semitronics Inc., 4242 Reynolds Dr. Hilliard, OH 43026. http://www.ohiosemitronics.com/

9. Berg, D.E., Rumsey, M.A., and Zayas, J.R., "Hardware and Software Developments for the Accurate Time-Linked Data Acquisition System," *2000ASME Wind Energy Symposium*, 200, p. 306.

10. Jones, Perry, Herbert J. Sutherland, and Byron A. Neal, "LIST/BMI Turbines Instrumentation and Infrastructure," SAND2001-1642 June 2001.

11. Citel Inc. Citel Inc., 1515 N W 167th Street - Suite 6-303, Miami, FL 33169. http://www.citelprotection.com/index.htm

12. Fiberplex, Fiberplex Inc,.10840-412 Guilford Road, Annapolis Junction, MD 20701. http://www.fiberplex.com/

13. Tower Systems, 17226 447th Ave, PO Box 1474, Watertown, SD 57201. http://www.towersystems.com/

14. MSC Software: http://www.mscsoftware.com/

15. Jonkman, J., "FAST", National Renewable Energy Laboratory website, July 2005, http://wind.nrel.gov/designcodes/simulators/fast/

16. Jonkman, J. & Buhl M., "Fast User's Guide", June 2005, National Renewable Energy Laboratory, July 2005, http://wind.nrel.gov/designcodes/simulators/fast/FAST.pdf, p. 51.

APPENDIX A

DETAILED DIAGRAMS OF THE METEOROLOGICAL TOWERS

As noted above, there are a total of four meteorological (met) towers used in this experiment, six are shown but the others were not used in this test. Their locations at the site are described in Figure 3. Tower nomenclature is also presented. This appendix describes in detail the position of the various instruments mounted on these towers.

Figure A-1 defines the symbols used on the met towers.

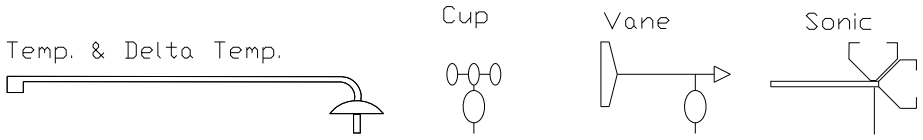

Figure A-1. Symbols Used on the Diagrams of the Meteorological Towers.

Center Meteorological Tower

A significant portion of instrumentation that characterizes the inflow is mounted on the center met tower. This tower is located directly in front, with respect to the prevailing wind, of the LWST turbine (see Figure 3). The instrumentation includes one sonic anemometer, one cup anemometer, one wind vane, temperature and differential temperature. The positions of all of these instruments are summarized in Figure A-2.

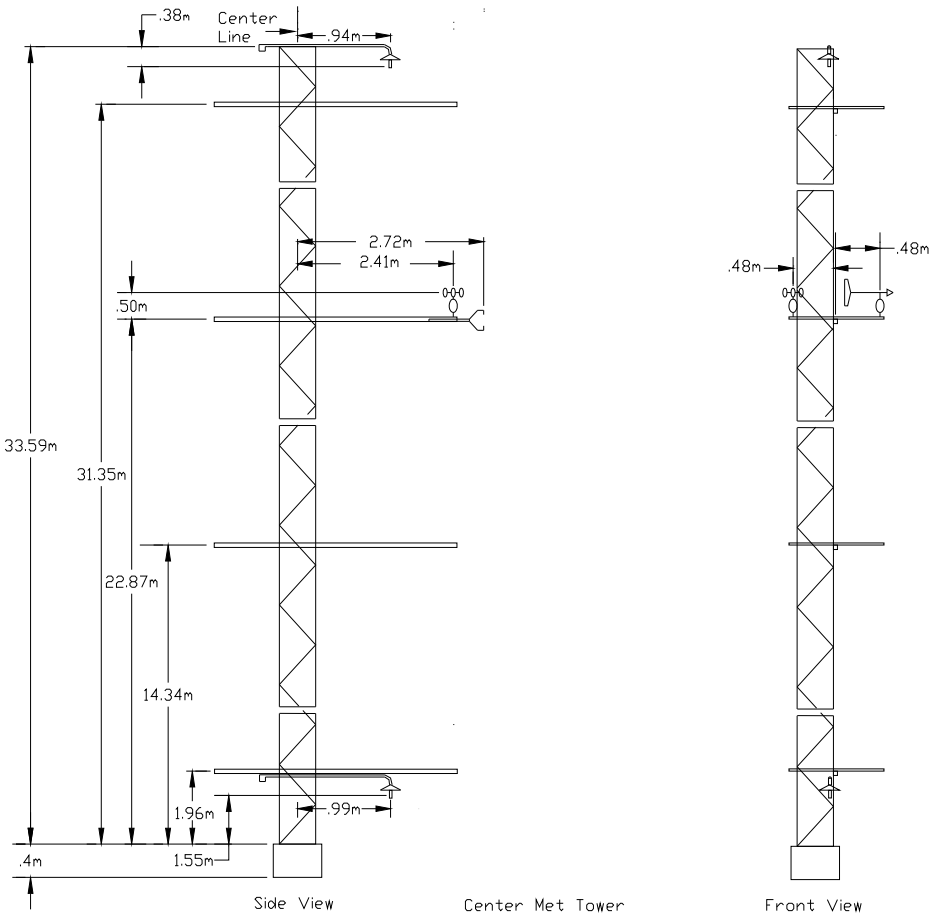

Figure A-2. Center Meteorological Tower.

North, South and Off-Axis Meteorological Towers

The remaining three towers (see Figure 3), have a cup anemometer and a wind vane mounted on their top. The position of these instruments is summarized in Figure A-3.

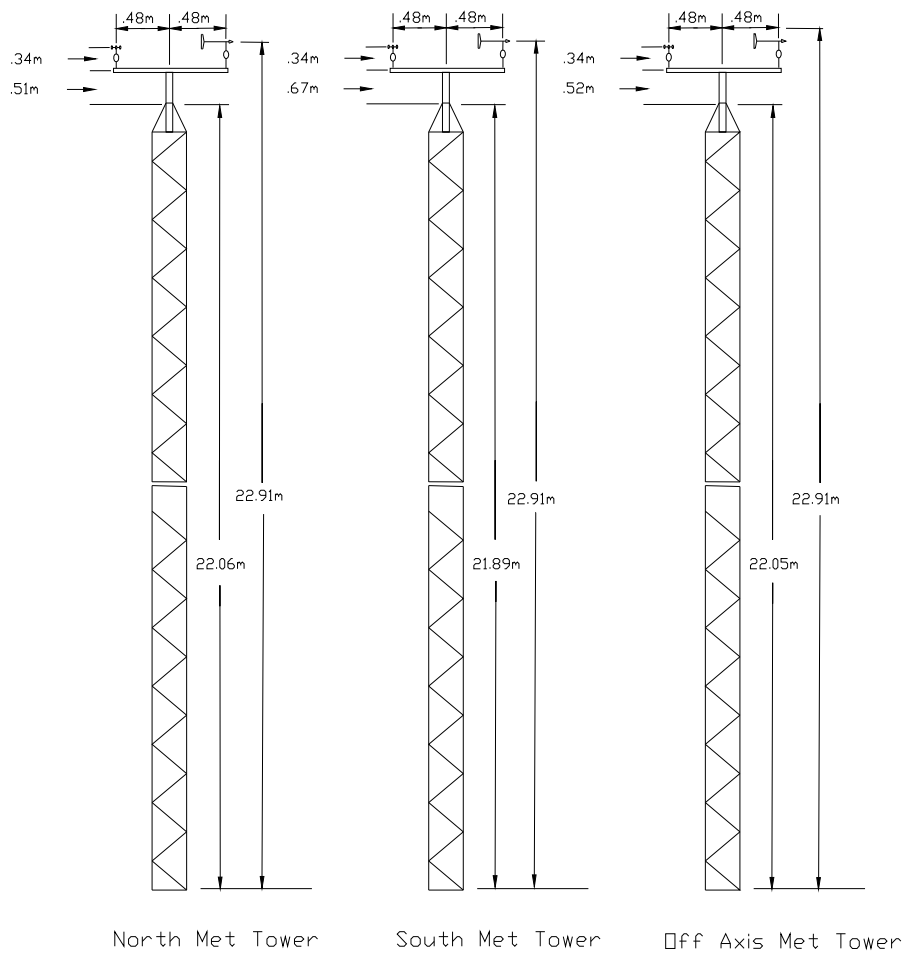

Figure A-3. North, South, and Off-Axis Meteorological Towers.

APPENDIX B

INSTRUMENTATION SPECIFICATIONS

A complete list of the instrumentation circuits is given in Tables 1, 2 and 3. This appendix describes the instruments, their specifications and their placement.

Met One Instrumentation

Met One Instruments Incorporated[2] wind speed, wind direction, temperature, differential temperature, and atmospheric pressure sensors are used here for the "standard" characterization of the inflow. The electronic packages that drive and process these sensors are rack-mounted units that are located in the instrument enclosure (see Appendix C).

Cup-and-Vane Anemometry

Cup Anemometer

Met One Model 1564B Wind Speed Transmitters[2] (cup) are used here for standard horizontal wind speed measurements. The accuracy of the instrument is ± 0.067 m/s or 1%, whichever is greater. The wind speed sensor uses highly reliable solid state optical sensing that is permanently aligned. The output of the sensor, a variable frequency signal, is sent to the signal processor. The output of the signal processor is an analog 0 to 5 VDC signal. For this installation, a 5-VDC output calibrates to a corresponding wind speed of 44.7 m/s (100 mph). The accuracy of the wind speed processor is ±0.1% of full scale.

The cup anemometers are hardwired through junction boxes at the base of the met towers to the instrument enclosure. The signal processors for all of the cup anemometers are mounted in the bottom section of the instrumentation rack in the instrument enclosure inside the instrumentation building (see Appendix C).

Wind Vane

Met One Model 1565C Wind Direction Transmitters[2] (vane) are used for the standard horizontal wind direction measurements. The accuracy of the instrument is ±2%. The output of the sensor is a constant amplitude variable phase signal that is sent to the signal processor. The output of the signal processor is an analog 0 to 5 VDC signal, with 5 VDC corresponding to a full rotation of the vane. The accuracy of the wind direction processor is ± 0.1% of full scale.

The vanes are hardwired through junction boxes at the base of the met towers to the instrument enclosure. The signal processors for all of the cup anemometers are mounted in the bottom section of the instrumentation rack in the instrument enclosure inside the instrumentation building (see Appendix C).

Mounting Hardware

On the Center Tower, the cup and vane are mounted on a cross arm that rotates 360° horizontally and adjust 0.52 m (1.5 ft) vertically. The cross arm is mounted at the end of an extendable boom arm made of aluminum tubing 5.08 cm (2 in.) square by 0.635 cm (0.25 in.) wall by 3.048 m (10 ft) long. The boom arm is mounted on the tower in a roller housing (Tower Systems Inc.)[13] that allows the boom arm to roll in and out of the roller housing. The arm is braced with 5.08-cm (2-inch) aluminum angle attached at the tower and clamped at about 1.22 m (4 ft) out on the arm (see Figure A-2).

On the other towers (North, South and Off-Axis), the cup and vane cross arms are mounted directly to the top of the tower (see Figure A-3).

Temperature Measurements

Absolute Temperature

The temperature is measured at approximately 1.6 m (5.1 ft) above ground level by a four-wire platinum resistance temperature detector (PRT), Met One Model No. 063-1.[2] The PRT produces a large output resistance change for a small input temperature change. The range of the PRT is ±50 °C with a quoted linearity of ±0.15 °C and an accuracy of ±0.1 °C. The output of the signal processor is an analog 0 to 5 VDC signal, with 0 volts corresponding to -50 °C and 5 VDC corresponding to 50 °C.

The temperature sensor is hardwired through a junction box at the base of the Center Tower to the instrument enclosure. The signal processor is mounted in the bottom section of the instrumentation rack in the instrument enclosure inside the instrumentation building (see Appendix C).

Differential Temperature

The differential temperature is measured between the top of the rotor [33.6 m (110 ft)], and the ground level [1.6 m (5.1 ft.)], with two four-wire PRTs, Met One Model No. 063-1[2] (see the discussion above; the lower differential temperature sensor is also the temperature sensor). The two signals are processed using a differential signal processor. The output of the signal processor is an analog 0 to 5 VDC signal, with 0 volts corresponding to -5 °C and 5 VDC corresponding to 15°C.

The temperature sensors are hardwired through a junction box at the base of the Center Tower to the instrument enclosure. The signal processor is mounted in the bottom section of the instrumentation rack in the instrument enclosure inside the instrumentation building (see Appendix C).

Mounting Hardware

The temperature sensors are mounted on the end a tubular arm with a solar shield over the sensor at about 1 m from the tower and aligned with the prevailing wind direction of 215° (see Figure 3). The temperature sensor is kept at ambient temperature by a 110-VAC fan at the opposite end of the tubular arm. Air is drawn over the sensor and exits at the fan end. The tubular arm is held in place by "U" bolts that attach it to the tower. The PRT is hardwired to a junction box at the base of the met tower and then wired to the instrument enclosure.

Barometric Pressure

The barometric pressure is measured at approximately 2.13 m (7 ft) above ground level, inside the instrument building. The instrument is a Yellow Springs Instruments Inc. Model 2014-75/1050.[4] The instrument range is 74.5 to 105 kPa with an accuracy of ± 0.125% of full scale.

The sensor is hardwired directly to the instrument enclosure. A Met One[2] signal processor is used to monitor this gauge. The Met One processor is mounted in the bottom section of the instrumentation rack in the instrument enclosure inside the instrumentation building (see Appendix C).

Sonic Anemometer

One Applied Technologies Incorporated Sonic Anemometer/thermometer[3] model SATI/3K is used here for the "detailed" inflow measurement. This unit measures three velocity components (two horizontal, U and V, and one vertical, W) and the sonic temperature. Its accuracy is ± 0.05 m/sec on wind velocity and ±1° above 2 m/sec on wind direction, ±0.05 °C on sonic temperature, and ±2° absolute temperature. Resolution is 0.01 m/sec on wind velocity, 0.1° on wind direction, and 0.01 °C on temperature. The sample rate is 200 Hz with 12 bit resolution digital output. The output of its analog signal processor ranges from -5 VDC to +5 VDC. For the U and V components of wind speed, 5 volts corresponds to a 50 m/s (111.85 mph) wind speed. For W, it corresponds to 15 m/s (33.55 mph).

The sonic anemometer is hardwired through junction boxes at the base of the met tower to the instrument enclosure. The signal processor for the sonic anemometer is mounted in the middle of the instrumentation rack (see Appendix C).

The sonic anemometer is mounted on the Center Tower on an extendable boom arm made of aluminum tubing 5.08 cm (2 in.) square by 0.635 cm (0.25 inch) wall by 3.048 m (10 ft) long. The boom arm is mounted at the tower in a roller housing (Tower Systems Inc.)[13] allowing for the arm to freely roll in and out. The arm is braced with 5.08-cm (2-in.) aluminum angle attached at the tower with "U" bolts and clamped at about 1.22 m (4 ft) out on the arm with a toggle clamp (see Figure A-2).

Strain Gauges

A total of 17 strain gauge circuits and two six-axis motion sensing units are used here to monitor the structural performance of the Micon turbine (see Figure 6). A complete list of the strain gauge circuits is given in Table 4. All of these circuits use full bridges built from strain gauges manufactured by Micro Measurements (Measurements Group).[5]

The strain gauge circuits use internal bridge card circuitry in the ATLAS II units.[1] This circuitry supplies both the excitation voltages and the balancing circuits for the strain gauge bridges. For the circuits used here, excitation voltages are ±5, ±3.75 or ±2.5 VDC. The monitoring circuits used multipliers of 2000, 1000, or 50. The choice of excitation voltage and multiplier for each circuit was based on the excited output of that circuit. Offsets for the monitoring circuits were set individually.

The strain-gauge circuits that are mounted to components of the rotor are hardwired to Windy, the rotor-based unit of ATLAS II.[12] Since the wire runs are relatively short, the excitation voltage can be monitored at Windy rather than at the bridge. The gauges mounted to the tower are hardwired to a GBU in the instrument enclosure. As this run is approximately 35 m (114.84 ft), the excitation voltage to each bridge was monitored at the "completion tabs" for the bridge, using the "six-wire" bridge circuit capabilities of the ATLAS II bridge circuit cards.

Blade Gauges

The 3X-100 blades were instrumented with strain circuits wired to measure bending stresses, one each in flap and edge directions at the blade root. Gauges were mounted and the spar cap and the leading and trailing edges. Additional gauges on one blade of the 3X-100 are at 25%, 50%, and 75% of span. The gauges used for these installations are dual-element, encapsulated 350-ohm gauges (WK-06-250PD-350) (see Figure B-1). The root gauges are mounted in the flap and edge configuration at 350 mm (13.8 in.) from the root flange. The flap gauges are mounted at the position of maximum thickness of the airfoil; at spanwise locations of 2550 mm (100.4 in.) from the root flange, 4500 mm (177.2 in.) from the root flange, and 6750 mm (266.1 in.) from the root flange. The strain gauge circuit for each set is wired as a full bridge with four active elements.

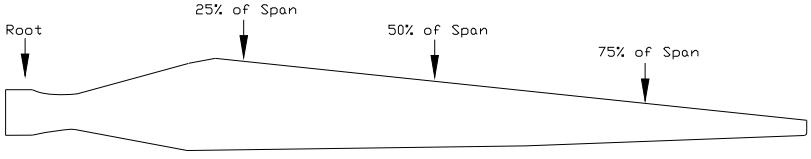

Figure B-1. Blade Strain Gauges.

The gauges are mounted internally to the blade and the wiring between the gauges and Windy is routed through the interior of the blades.

Hub Gauges

The hub on the Micon turbine was instrumented with six bending strain gauge circuits: one each used to measure the flap and edge bending in each of the three blade mounting arms (see Figure B-2). Dual-element, encapsulated 350-ohm gauges (WK-06-250PD-350) were used for these bending bridge circuits. The strain gauges were located on the exterior of the hub at approximately 0.165 m (6.5 in.) from the blade-mounting flange. This dimension corresponds to 0.435 m (17.1 in.) from the centerline of the main shaft.

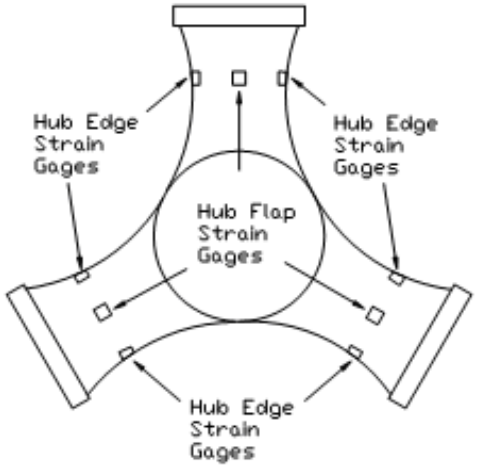

Figure B-2. Hub Strain Gauges.

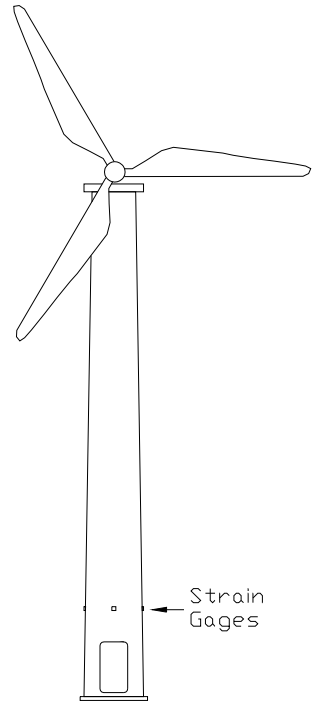

Figure B-3. Tower Strain Gauges.

Tower Bending

Tower bending was measured with dual–element, encapsulated 90° tee rosette 350-ohm gauges (WK-06-250TM-350). One set measured fore-aft bending and the other side-to-side bending. They were aligned with the prevailing winds at 215°. The gauges were mounted inside of the tower at about 3.9 m (154 in.) above the turbine base (see Figure B-3).

Accelerations Measurement System

The nacelle was instrumented with one micro-machined (MEMS) device six-axis measuring system. It measured fore-aft, side-to-side, and up-down accelerations with three MEMS accelerometers and measured pitch, roll, and yaw rates with three angular rate sensors consisting of vibrating ceramic plates that utilize the Coriolis force to output angular rate independent of acceleration. The instrument was a Crossbow IMU300CC-100,[6] and was located on the nacelle frame next to the gearbox.

The accelerometers were located in a small junction box on the nacelle frame next to the gear box on the turbine (see Figure B-4). The units were hardwired through a junction box located in the base of the turbine to the instrument enclosure.

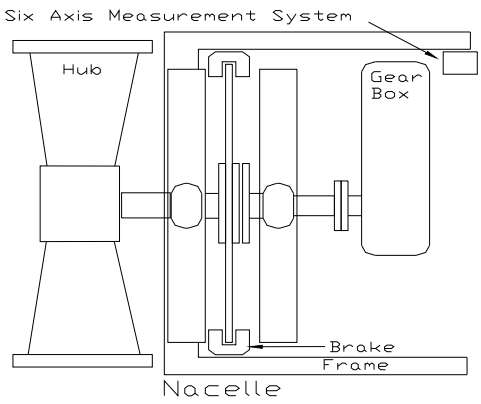

Figure B-4. Acceleration Measurement System

Additional Instruments

Yaw Position

The angular position of the nacelle, i.e., the yaw position, was measured with a brushless rotary encoder, model number HSTDCC-PB16S-SE, Computer Conversions Corporation.[7] Its resolution was 0.025% with an accuracy of ±12 arc-minutes. Uni-directional repeatability was 0.028%; bi-directional was ± 0.028%. Output ripple was 5 millivolts peak to peak (P-P) maximum.

The encoder was mounted to the top of the yaw drive gear box inside the nacelle. Pulleys, connected using a toothed belt, were used to attach the encoder to the yaw drive (see Figure 11). The size of the pulleys was chosen to yield a yaw position that is directly proportional to the output of the encoder.

The encoder was hardwired through a junction box in the bottom of the tower to a servo-loop signal processing decoding card in the instrument enclosure. The decoder card converted the angle signals from DC signal voltage. The output voltage ranged from 0 to 5 during a revolution of the nacelle. Excitation for the encoder was ±15 VDC. The power supply and the signal processing decoder were located near the bottom of the instrument enclosure (see Appendix C).

Rotor Azimuth and Velocity

The angular position and velocity were measured by a brushless rotary encoder, model EVSTDCC-PB16VIC-SIRPS, manufactured by Computer Conversions Corporation.[7] Uni-directional repeatability was 0.028%; bi-directional was ± 0.028%. Output ripple was 5 millivolts P-P maximum. A 5-volt output corresponded to an angular velocity of one rps with an accuracy of 0.1% over one revolution

The encoder was mounted to the nacelle near the front of the gear box (see Figure 11). Sprockets, connected with a roller chain, were used to attach the main shaft to the encoder. The size of the sprockets was chosen to yield a rotor position that is directly proportional to the output of the encoder.

The encoder was hardwired through a junction box in the bottom of the tower to a servo-loop signal processing decoding card in the instrument enclosure. The decoder card converted the DC signal voltage to an angle signal. The signal for rotary position ranged from 0 to 5 during a revolution of the blades. Excitation for the encoder was ±15 VDC. The power supply and the signal processing decoder were located near the bottom of the instrument enclosure (see Appendix C).

Power

The power produced by the turbines was monitored using a model GWV5-006AY precision WATT/VAR transducer by Ohio Semitronics Inc.[8] The instrument was designed for three-phase operation at 380-550 volt, 0-100 amp, and 0-80 KV/VAR. The instrument measured three-phase voltage, current, total power and volts amps reactive (VAR). For this installation, the unit was only used to monitor the total power produced by the turbine. A 5-VDC output from the transducer was equal to 600 VAC and 4000 WATT/VAR with an accuracy of ± 0.2% of reading and ± 0.05% full scale.

The non-contact current transformers (coils), the primary sensors used by this instrument, were placed around the three-phase, 480-volt power wires that connects the turbine generator to the grid. The coils, located inside the turbine control panel at the base of the turbine, were hard-wired to a monitoring unit also located inside the control panel. The units were hardwired through the junction box in the base of the turbine to the instrument enclosure.

Control Switch

The Control Switch was a signal that indicated when the turbine is up to speed, producing power and connected to the utility grid. Using the controller signal that connected the generator to the grid, an auxiliary relay was used to supply an on/off signal. A 5-VDC power supply output was switched through the relay to provide the on/off signal to the data acquisition system. The relay and the power supply were located in the turbine control junction box in the base of the turbine tower.

APPENDIX C

WIRING DIAGRAMS

Instrument Enclosure

The instrument enclosure was a large metal junction box 1.83 m (6 ft) wide by 1.83 m (6 ft) high by 0.61m (2 ft) deep with two doors and was located in the instrument building. This unit was designed so that it can be utilized at other wind turbine sites by disconnecting the input signal lines at the lightning protection interface. It then can be transported to another site with all the interconnections intact and then be reconnected to the instrumentation at the new site. It is shown in Figure 13.

AC Power Supply

AC power was provided to all instrumentation via an uninterruptible power supply (UPS).

DC Power Supplies

The ATLAS II power and the ATI power were provided by two ±12-volt power supplies. The Crossbow Acceleration measurement system was powered by a 15-volt power supply. The yaw position, rotor velocity, rotor position encoders and their electronics boards were powered by a ±15-volt power supply (see Figures C-1 and C-2).

Figure C-1. Power Supplies and Back Panel of the Instrument Enclosure.

Figure C-2. AC Power Distribution in the Instrument Enclosure.

Lightning Protection

Lightning protection was provided for all of the instrumentation and electronic equipment used at the site to protect the hardware. The majority of the lightning protection was mounted in the instrument enclosure (see Figures C-3 and C-4). All of the data and signal lines had shield wires that are grounded to a common ground before the data and signal lines were passed through the lightning protection circuit.

Citel Inc.[11] manufactured the lightning protection units. Each unit consisted of a base circuit board that can hold up to eight plug-in modules. Each module protected two pairs of wires. The module circuitry incorporated a high-speed gas tube/avalanche diode with a one-nanosecond surge arrest time. They can dissipate up to 10,000 amperes. Modules come with clamping voltages of 6 and 12 volts, and they can be interspersed about the circuit board as required.

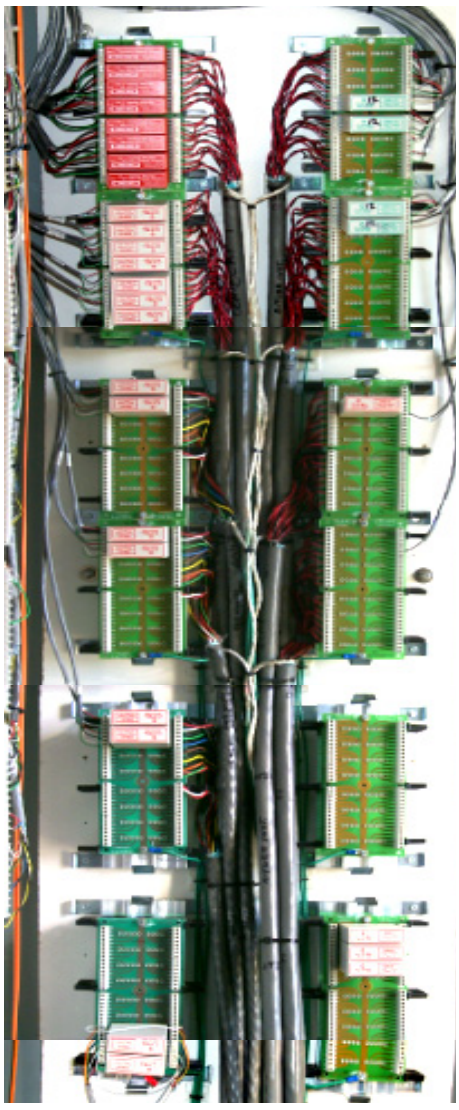

Figure C-3. Lightning Protection Panels in the Instrument Enclosure.

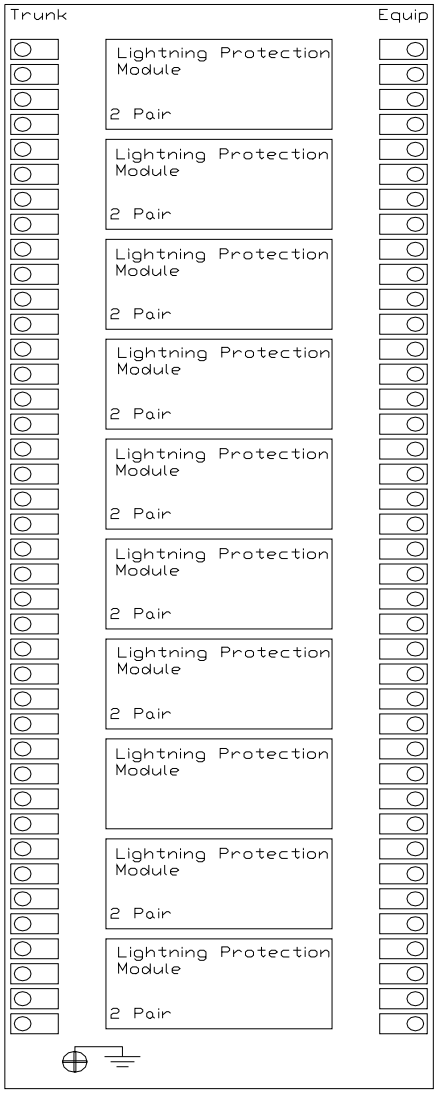

Figure C-4. Typical Lightning Protection Circuit Board.

Instrument Rack

The slide out rack (see Figures C-5 and C-6) housed the ATLAS II Ground Based Unit, the Met One[2] signal processors and power supply racks, and the ATI sonic anemometers digital-to-analog converters. Power strips located in the bottom of the rack provided AC power. The rack was on slides that allowed the rack to move in and out 24 inches to gain access to the front and back of the rack and the to AC power distribution located on the left wall of the enclosure.

Figure C-5. Front View of the Instrument Rack.

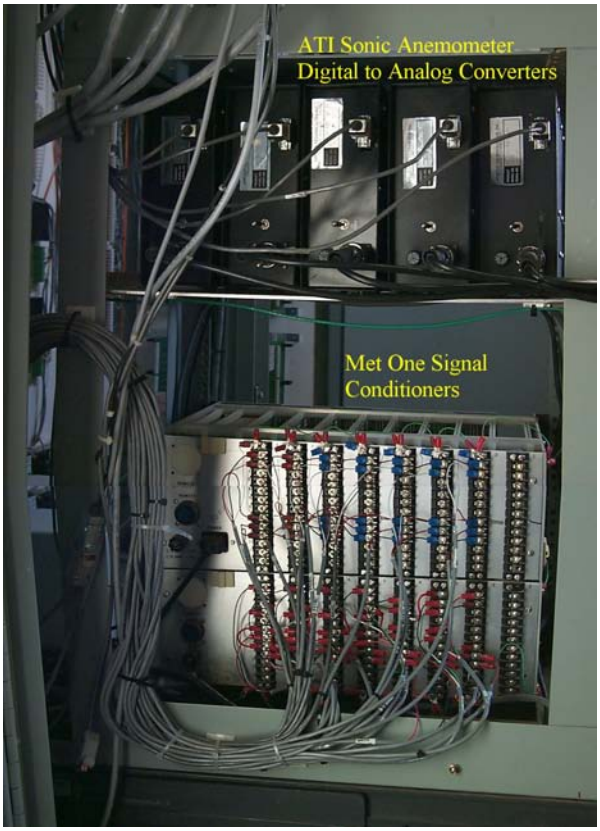

Figure C-6. Rear View of the Instrument Rack.

DISTRIBUTION

Cecelia M. Poshedly (3)
Office of Wind and Hydropower Technologies
EE-2B Forrestal Building
U.S. Department of Energy
1000 Independence Avenue SW
Washington, DC 20585

Dennis H. Lin
Office of Wind and Hydropower Technologies
EE-2B Forrestal Building
U.S. Department of Energy
1000 Independence Avenue SW
Washington, DC 20585

Derek Berry
TPI Composites, Inc.
373 Market Street
Warren, RI 02885-0328

Steve Lockard
TPI Composites, Inc.
373 Market Street
Warren, RI 02885-0367

Scott Hughes
NREL/NWTC
1617 Cole Boulevard, MS 3911
Golden, CO 80401

Jeroen van Dam
Windward Engineering
NREL/NWTC
1617 Cole Boulevard
Golden, CO 80401

Michael Robinson
NREL/NWTC
1617 Cole Boulevard
Golden, CO 80401

Daniel Sanchez
U.S. Department of Energy
NNSA/SSO
P.O. Box 5400 Mail Stop: 0184
Albuquerque, NM 87185-0184

Brian Smith
NREL/NWTC
1617 Cole Boulevard
Golden, CO 80401

Herb Sutherland
1700 Camino Gusto NW
Albuquerque, NM 87107-2615

Robert W. Thresher
NREL/NWTC
1617 Cole Boulevard
Golden, CO 80401

R. Nolan. Clark
USDA Agricultural Research Service
PO Drawer 10
Bushland TX 79012

B. Neal
USDA Agricultural Research Service
PO Drawer 10
Bushland TX 79012

A. Holman
USDA Agricultural Research Service
PO Drawer 10
Bushland TX 79012

Mansour Mohamed (3)
3TEX Inc.
109 MacKenan Dr
Cary, NC 275111

NWTC Library (2)
NREL
1617 Cole Boulevard
Golden CO 80401

Internal Distribution:

MS 0557	T. J. Baca
MS 0557	T. G. Carne
MS 1124	D. E. Berg
MS 1124	T. D. Ashwill
MS 0557	D. T. Griffith
MS 1124	J. Stinebaugh
MS1124	R.R. Hill
MS 0718	P. L. Jones
MS 1124	B. Karlson
MS 1124	D. L. Laird
MS 1124	J. Ortiz
MS 1124	M. A. Rumsey
MS 1124	W. Johnson (2)
MS 1124	J. Paquette
MS 1124	P. S. Veers
MS 1124	J. Zayas
MS 0899	Technical Library, 9536 (Electronic)


Sandia National Laboratories